University of Ottawa
Faculty of Medicine
Department of Cellular and Molecular Medicine

Neuroscience Master's Thesis

Identifying Unique Coding Strategies Between Mossy Fibre and Interneuron Synapses

Author
Yishan MA
Publishing Name: Sandy MA YISHAN

Supervisor
Katalin TÓTH

Committee Members
Leonard MALER
Jean-Claude BÉÏQUE

A Thesis Submitted in Partial Fulfilment of the Requirements for the Degree of Master of Science in Neuroscience

Abstract

Animals use spatial navigation to move about their environment and the hippocampus is the centre of processing of spatial information. We want to understand how the mossy fibre (MF) of the hippocampus (HPC) decodes inputs from the entorhinal cortex (EC) and contributes to spatial memory processing. MF terminals have unique anatomical features that connect dentate gyrus granule cells (DG; DGGC) to CA3 pyramidal cells (CA3PC), along with single release site extensions that synapse onto CA3 stratum lucidum interneurons (SLIN). Using whole-cell patch-clamp electrophysiology, we recorded from MF-CA3PC synapses and stimulated patterns that differed in frequency, but the number of stimuli remained the same. We discovered a novel coding strategy, termed AP Counting. AP Counting happens when the synapse responds to the number of stimuli, irrespective of their frequencies. It remains unknown whether this is a uniform feature of presynaptic elements or of various postsynaptic elements. Therefore, is the same coding strategy, AP Counting, preserved between MF-SLINs? Preliminary findings revealed that MF-SLIN coding strategies to be different from the ones employed at MF-CA3PCs. Thereby, we separated the three populations by coding strategy and named them SLIN population 1 (SLIN1), SLIN population 2 (SLIN2) and SLIN population 3 (SLIN3). SLIN1 and SLIN3 employed a rate coding strategy, while SLIN2 was insensitive to different frequencies. In conclusion, MF-SLINs utilise distinct coding from MF-CA3PCs, namely, rate coding, and frequency insensitivity. These two different ways of processing (EC) contribute to the complexity of the neural dynamics of the DG-CA3 network. In order to understand the greater impact of these two types of synapses, we would use computational modelling to study the dynamics of the DG-CA3 network.

Table of Contents

List of Abbreviations

aCSF	Artificial Cerebrospinal Fluid
AMPA	α-amino-3-hydroxy-5-methyl-4-isoxazole-propionate
AMPAR	α-amino-3-hydroxy-5-methyl-4-isoxazole-propionate Receptor
AP	Action Potential
CA1/CA3	*Cornu Ammonis* 1/*Cornu Ammonis* 3
CA3PC	CA3 Pyramidal Cell
CA3SLIN	CA3 Stratum Lucidum Interneuron
CP-AMPAR	Calcium Permeable AMPAR

CI-AMPAR	Calcium Impermeable AMPAR
DG	Dentate Gyrus
DCG-IV	(1R,2R)-3-[(1S)-1-amino-2-hydroxy-2-oxoethyl]cyclopropane-1,2-dicarboxylic acid
EC	Entorhinal Cortex
EGTA	Ethylene Glycol Tetraacetic Acid
EPSC	Excitatory Postsynaptic Current
GABA	γ-Aminobutyric acid
MFA	Mossy Fibre Axon
MFB	Mossy Fibre Bouton
MFF	Mossy Fibre Filopodia
mGluR2/3/7	Metabotropic Glutamate Receptors Group 2/3/7
NBQX	2,3-dihydroxy-6-nitro-7-sulphamoyl-benzo(F)quinoxaline
NMDA	N-methyl-D-aspartate
NMDAR	N-methyl-D-aspartate Receptor
PBS	Phosphate Buffer Solutions
PFA	Paraformaldehyde
PP	Paired Pulse
PPR	Pair Pulse Ratio
SLIN	Stratum Lucidum Interneuron

Acknowledgements

I want to thank everyone who has supported and contributed to the completion of my MSc thesis. Firstly, I am grateful to my supervisor, Katalin Tóth. You amazed me with your graciousness and mentorship of my mistakes. I promise, I will always remember V= IR.

To my committee members, Jean-Claude Béïque and Leonard Maler, thank you for your support. JC, for the fun chats on twitter science culture and Len, for always having cool science to share! To Diane Lagace, Richard Naud, Greg Silasi, thank you for joining my thesis committee - it was good to have you at the end of my MSC journey.

For our lab manager, Dr. Lynda David, who despite not showing up for our first hangout because (she took a bus to the other side of town), you have since shown up for me countless times.

The other neuroscience student, or the lunch crew, the lunches were always filled with chaos and fun, that made long days shorter! Climbing was always good times and splendid laughs. For the pineapple group, the people I met at CAN, and previous labmates - thank you for getting me through!

Thank you to the leadership of the Faculty of Medicine and to the University of Ottawa staff that support research. For the ACVS staff, human rights office, tech support, accessibility, waste management, and security, thank you. Your work is often invisible, but because of your efforts, researchers like me could do our experiments with each wave of the pandemic. We made it.

Lastly, I would like to acknowledge the mice used in this thesis. The payment of their lives gave me the results that will ultimately contribute to our collective understanding of neuroscience. I hope we use the data to make the world better. Thank you.

Author Contributions

The AP Counting experiments was conducted by Simon Chamberland and published in his 2018 paper (Chamberland et al., 2018). The results that provided the framework for my MSc work were carried out by Maxime Houtekamer and Simon Chamberland. They recorded and analysed the electrophysiology data. All other electrophysiology data, analysis, or custom software were done by me.

Preface: Thesis Chapters

The introduction will be divided into three segments: Chapter 1A, 1B, and 1C.

Chapter 1 Part A: The Discovery of the Hippocampus
The first part will take a deep dive of the hippocampus, with a bit more focus on the history. I will cover the discovery, drawing, and naming of the hippocampus. It is a bit unorthodox to cover history so extensively in a neuroscience MSc thesis, but I found it absolutely fascinating. I started exploring the history because I was wondering why the CA3 was almost never spelled out, despite being an acronym. CA3 is almost as ubiquitous in neuroscience as CIA is in spy books or GPS for navigation. But what does the CA3 stand for? I will cover that. In short, curiosity blossomed into Chapter 1 Part A. I thought if I learned something from observing a big-picture view of the hippocampus, someone else might too!

Chapter 1 Part B: Neurotransmission and Plasticity
The section will be more similar to a traditional thesis introduction. I will cover the fundamental concepts of neuroscience, membrane potential, action potentials, vesicular transport, and plasticity. I will discuss the basics of electrophysiology to introduce the mechanisms of hippocampal neurotransmission.

Chapter 1 Part C: Hippocampal Circuits: CA3 Synapses and Dynamics
Finally, I will give an overview of mossy fibre anatomy and synaptic plasticity mechanisms. I will specifically examine all the previously introduced concepts and apply them in the framework of mossy fibres. This will establish the literature, previous experiments, and precedence for my work in Chapter 2.

Chapter 2: Hypothesis, Results, and Discussion
In this chapter, I discuss how we investigate neurotransmission at CA3 synapses by exploring their coding mechanisms. I show that MFF-SLIN synapses demonstrate 3 varied coding strategies, different from the AP Counting at MFB-CA3PC synapses previously published in our lab. I show that these differences in short-term plasticity mechanisms could apply 3 methods of applying feed-forward inhibition to downstream CA3PCs.

Chapter 1

Part A | The Discovery of the Hippocampus

Introduction: The Discovery and Naming of the Hippocampus

1A.1 | Discovery of the Hippocampus

The first description of the hippocampus was published by Italian anatomist and surgeon Julius Caesar Arantius (Giulio Cesare Aranzio, Arantius; 1510 - 1589), in his 1587 book entitled *"Observationes Anatomicae: De Humano Foetu Liber*" or "Anatomical Observations: Book on the Human Foetus" (Arantius, 1923; Bir et al., 2015; Engelhardt, 2016). He described the hippocampus as "a white prominence" that rises up from the ventricles. The structure resembled a "white silkworm", "horse-caterpillar", or a "seahorse" (Arantius, 1923; Bir et al., 2015; Lewis, 1923; Engelhardt, 2016). In later editions of his book, Arantius named the brain structure "hippocampus" due to its resemblance to the shape of a seahorse (Arantius, 1923; Bir et al., 2015; Lewis, 1923). The name was derived from the Greek words "*hippos"* meaning horse and "*kampos*" meaning sea monster (Bir et al., 2015).

1.A.2 | Naming the Hippocampus

Another name that has been used to refer to the hippocampus is "*Cornu Ammonis*" or Latin for "Ammon's horn." In 1732, Danish anatomist Jacob Winslow referred to the hippocampus as a "ram's horn." Later, his colleague, Garengeot changed the term to "*Cornu Ammonis*" (Bir et al., 2015), referring to the Egyptian deity, Ammon (or

Amun). Ammon was often depicted with having ram's horns on his head. The name in its long-form "*Cornu Ammonis*" is no longer used to refer to the hippocampus. Instead, the short-form of "*Cornu Ammonis*" (CA) is the standard naming practice used to identify the subsections of the hippocampus Cornu Ammonis 4, 3, 2, 1 (CA4, CA3, CA2, and CA1; (Bir et al., 2015).

The term "hippocampal formation", coined by O'Keefe and Nadel in 1978 paper "The Hippocampus as a Cognitive Map". They defined the "hippocampal formation" to include the hippocampus proper (CA4-CA1) and its adjacent structures, the dentate gyrus and subiculum. The authors argued the complex network of these structures was essential for the creation of cognitive maps (Andersen et al., 2009; O'Keefe & Nadel, 1978). In many instances the entorhinal cortex is also included due to its importance in encoding spatial information. For that reason, the hippocampal formation is most often and commonly used in the spatial navigation literature. Although many names have been used throughout history to describe the hippocampus, they are no longer commonly cited in modern literature (Bir et al., 2015). The one that is most used, "hippocampus", is the one that remains dominant in the field today.

1.A.3 | Visualisation of the Hippocampus

Although Arantius was the first to publish a description of the hippocampus, he did not include any visual representations of the structure in his book (Engelhardt, 2016). In 1729, German anatomist and botanist Johann Georg Duvernoy (*Johannes Georgius Duvernoi*; 1648 - 1730) published the first drawing of the hippocampus within the brain in his article entitled "*De Sinibus Cerebri*" or "On sinuses [ventricles, cavities] of the brain (Engelhardt, 2016)". American neuroscientist James T. M'Carthy (1851 - 1929) used meticulous dissection techniques to provide a comprehensive description of the anatomy of the hippocampus (M Carthy, 1898). However, these drawings are all often overshadowed by the illustrations of Spanish neuroscientist Santiago Ramón y Cajal (1852 - 1934). In his books "*Manual de histología normal y técnica micrográfica*" or "Manual of Normal Histology and Microscopic Technique (1890)" and "Textura del Sistema Nervioso del Hombre y los Vertebrados" or "Texture of the Nervous System of Man and the Vertebrates (1899-1904)", he provided detailed descriptions of the structure and organisation of the nervous system (Garcia-Lopez et al., 2010). He accompanied the description of each system, ranging from the visual system to the hippocampus, with intricate drawings and circuit diagrams of the region (Figure 1; Klein, 2017).

He used Golgi staining techniques to produce visual representations of cellular components (Klein, 2017). He noted that the hippocampus consisted of layers of densely packed cells with distinct patterns of connections to other parts of the brain. In his later books, he proposed the hippocampus played a role in processing sensory information. The illustrations are known not only for their intricate detail, but also accurate visualisation of the anatomy at both the structural and cellular level (Ramón y Cajal, 1899; Sotelo, 2003). All these publications are considered seminal contributions and are widely cited references in the field of neuroscience. Due to his extensive contributions to our understanding of the hippocampus and its function, Ramón y Cajal is often cited as the modern discovery of the hippocampus. He won a Nobel Prize for Physiology or Medicine in 1906 for his work in establishing the neuron as the basic unit of the central nervous system.

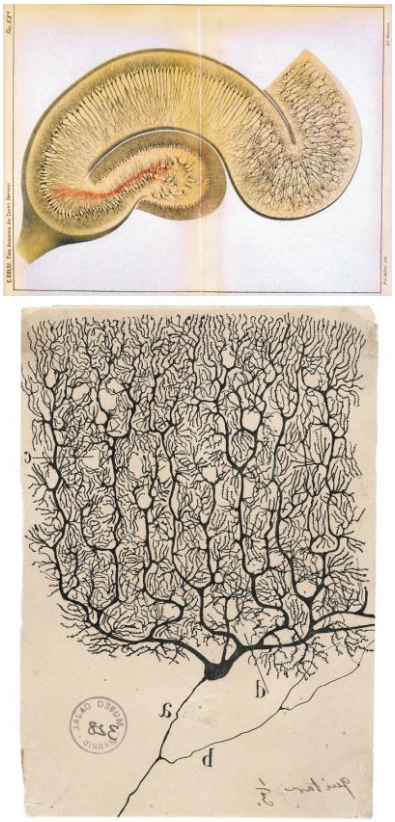

Figure 1 | *Top*: Golgi developed the Golgi staining method to reveal neural structures, this example shows the pyramidal neurons of a rabbit hippocampus (Golgi, 1885). *Bottom*: Ramón y Cajal used the Golgi method to intricately illustrate the structure of the nervous system, like this human cerebellar Purkinje neuron (Ramón y Cajal, 1909)

Introduction: Early Hippocampal Experiments in Humans

Some of the earliest experiments on the brain date back to five millenia (Asadi-Pooya & Rostami, 2017). Trepanation, one of the earliest neurosurgery techniques, was recorded to date back to 10 000 BC (Nikova & Birbilis, 2017). It was used to treat anything from headaches to seizures to bad spirits. In the 1930s, Canadian neurosurgeon Wilder Penfield (1891 - 1976), developed a more targeted surgical approach to treat seizures. The “Montreal Procedure” involved using a probe to deliver small currents to awake patients. From their responses, he could locate the epileptic brain tissue and investigate the region’s function (Kumar & Yeragani, 2011; Penfield & Gage, 1933). After the tissue was removed, he would assess the functional differences in patients post-surgery. He concluded this targeted approach was more effective at treating patients with epilepsy.

During one of Penfield's surgeries, he stimulated the temporal lobe of his patients and they told him about a specific memory in vivid detail. He suspected the temporal lobe to play an important role for the storage of past experiences (Kumar & Yeragani, 2011). He was able to confirm his suspicions when two of his patients F.C. and P.B. developed severe amnesia after surgery. Both patients received unilateral lobectomies to the temporal lobe to treat severe epileptic seizures. This was an unexpected outcome (Penfield & Milner, 1958). He worked with Donald Hebb's student, Brenda Milner to study the two patients in depth. Together, they developed tests to evaluate their memory deficits and cognitive function (Penfield & Milner, 1958; Squire, 2009).

1A.4 | H.M.

Milner and Penfield presented their findings at a conference. William Scoville, a neurosurgeon in Connecticut, USA, called Penfield after the conference to discuss a patient who had similar memory impairments. The patient's name was H.M. (Squire, 2009). H.M. developed epileptic seizures at a young age after a bike accident. Although he took strong anticonvulsant medications, by the time he was 27 in 1953, he was no longer able to maintain a job or a normal life (Scoville & Milner, 1957). Scoville surgically removed a large portion of both temporal lobes, including parts of the amygdala and uncus (Squire, 2009). Scientists have since used magnetic resonance imaging to characterise the brain of H.M. and the region the lobectomy was performed (Corkin et al., 1997). Upon recovery, H.M. started to demonstrate memory deficits, worse than the ones described in Penfield's two patients, F.C. and P.B. (Penfield & Milner, 1958). Dr. Milner went to Connecticut to evaluate patient H.M. 's memory deficits. She would spend the next 4 decades with her colleagues studying H.M.

1A.5 | Main findings from H.M.

H.M. demonstrated deficits more severe than patients F.C. and P.B. He could remember memories from before his surgery, but not people he had just met a few minutes ago. Dr. Milner and her team published several papers describing the formal memory tests they conducted on H.M. (Milner, 1959, 1962, 1966; Milner et al., 1968; Scoville & Milner, 1957; Squire, 2009). The main findings can be summarised into the following four points:

1) *Short-term memory is impacted after temporal lobectomy*. He cannot remember an event from a few minutes ago and regularly restarted conversations that had recently occurred (Scoville & Milner, 1957).

2) *Working memory remains intact after temporal lobectomy*. During a conversation, he could not remember the beginning of the conversation, but he could hold the conversation while it was happening (Milner et al., 1968).

3) *Long-term memory is not stored in the hippocampus*. H.M. could recall events from before his surgery, even from his early childhood, but nothing after - he had anterograde amnesia (Corkin, 1984).

4) *Procedural memory is separate from declarative memory*. Despite having no memory of learning the task, H.M. mastered the complicated Mirror-Tracing Task (Figure 2; Milner, 1962).

These results were foundational to the study of memory, creating the early framework for our current system of memory types.

At the time, Milner's discoveries were initially controversial. The results from H.M. found that the centre for memory storage was a separate function from the intellect and perception (Scoville & Milner, 1957). This contradicted previous findings that memory was located in the frontal cortex and involved directly with intellectual functions (Lashley, 1929; Squire & Wixted, 2011). However, with more experimentation, the temporal lobe was accepted as the centre for memory. From this seminal paper, researchers were able to come up with theories that describe multiple memory systems (Atkinson & Shiffrin, 1968). Milner's paper is still highly cited today (10,637 Google Scholar citations at the time of writing in May 2023).

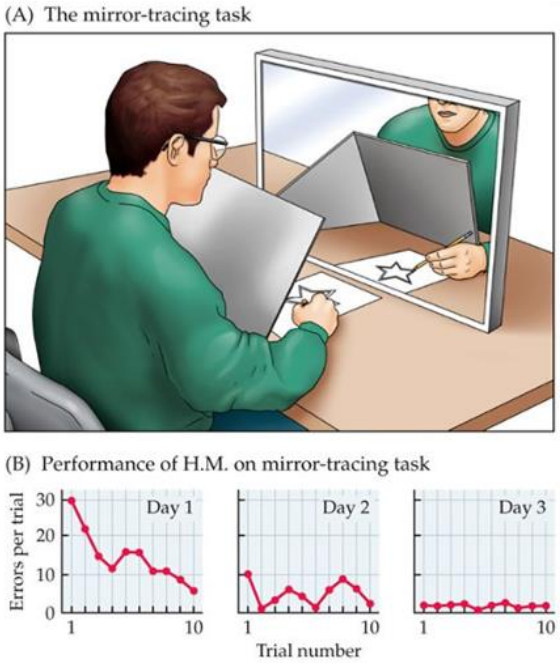

Figure 2 | The mirror tracing task. After his surgery, H.M. was taught to trace the mirror image of a star. On day 1 he struggled with the task, but improved with practice. Despite

Chapter 1

Part B | Neurotransmission and Plasticity

Introduction: Basic Introduction to Neurotransmission

1B.1 | Memory at the Cellular Level

In the previous chapter, I covered the history of the hippocampus. I reviewed the early human hippocampal experiments that established the hippocampus as playing a central role in human memory. However those studies lead to more questions: *What are the neuronal circuits involved with memory? How do these neurons transmit information to generate memories?* These questions will be the focus of Section 1B.7.

Before I can answer these questions, I must give a brief introduction to basic concepts of neuroscience, such as: *What is a neuron? How do neurons communicate? What are the mechanisms for neurotransmission?* I will discuss these questions with a focus on cellular electrophysiology, the main method of my thesis research. Then in Chapter 1 Part C, I will introduce the hippocampal formation, specifically the hippocampal circuits with more detail. Additionally, I will examine the experiments that answered those earlier questions and *What role does the hippocampus play in encoding memories?* Lastly in Chapter 1 Part C.3, I will take a deep dive into discussing mossy

fibre synapses. I will investigate their unique anatomy, synaptic properties, and the role they play in information transfer in the hippocampus. These sections will provide the reader with the necessary introduction prior to presenting the work I performed for my thesis in Chapter 2.

1B.2 | Parts of a Neuron

What is a neuron? A neuron, or a nerve cell, is the basic and functional unit of the central nervous system. Neurons communicate throughout the body by way of action potential, or brief electrical signals created by changes in neuronal membrane potential. Neurons, like people, come in many shapes and sizes. Despite their diversity, neurons share 3 common components: 1) dendrite 2) cell body 3) axon (Molnar & Gair, 2015a). The dendrites are the input sites of the neuron, receiving signals from other neurons. They integrate the electrical pulses from connected cells. Cell bodies contain the nucleus and all the other organelles required for maintaining normal cellular function. Meanwhile, axons project away from the cell body and carry signals to other neurons. The space between two contacting neurons is called a synapse (Molnar & Gair, 2015a). The synapse is formed by two parts: the pre-synaptic component, which are the terminals of axons and the post-synaptic side being the dendritic boutons.

Neurons send signals across the synapse by electrical (electrical synapse) or chemical (chemical synapse) transmission, or a combination of both (Purves et al., 2001b). Electrical synapses communicate directly with each other via gap junctions that flow ions from one neuron into another. This flow of ions is bidirectional. Chemical synapses communicate by neurotransmitter transmission: sending a molecule from one cell to another, across the synapse. We will only discuss the mechanisms of chemical transmission in detail.

The neuron, like all cells, separates intra- and extra- cellular space with a lipid bilayer (Westra et al., 2021). The lipid bilayer at neurons contains all the normal cell signalling molecules: phospholipids, integral membrane proteins, and protein channels. However, the cell membrane of dendrites, axons, and the extracellular space between neurons (i.e. synapse), is highly specialised for neural function. The axon is poised with specific channels to propagate action potential (AP) down to its terminal (Molnar & Gair, 2015b). Axon terminals have unique vesicular proteins and signalling pathways for pre-synaptic transmission. Dendrites contain receptors to receive transmission across the neighbouring synapses to relay to the soma. We will first discuss how axons transmit APs, then we will cover the mechanisms of how dendrites receive them.

1B.3 | Basics of Neurotransmission: Action Potential

How do neurons communicate? How does an AP propagate? To understand how to talk to one another, we must examine how an AP propagates down an axon. When a neuron is not active, the membrane potential of the cell is negative at approximately -70 mV. This difference in voltage is generated by varied intra- and extra- cellular concentrations of sodium (Na^+), potassium (K^+), chloride (Cl^-), and organic anions and maintained by voltage-gated and leaky channels. This baseline is called the resting membrane potential and is well described by Molnar & Gair, 2015b. The resting membrane potential can vary across cell types, but -70 mV is generally accepted as the baseline. Upon receiving excitatory inputs from the dendrites, the neuron starts to depolarize, increasing the membrane potential. Once the membrane potential reaches the threshold potential, approximately -55 mV, an AP is fired. APs are all-or-nothing, so when the threshold potential is reached, a neuron depolarizes. The peak of an AP is approximately +40 mV and the beginning of repolarization and the refractory period. Na^+ channels close and cannot open during this time. Meanwhile, voltage-gated K^+ channels open, letting K^+ ions to leave the cell, hyperpolarizing the membrane before reaching the membrane resting potential again. Return to the baseline means the neuron is reset and ready to fire again. Action potential signals the fundamental carriers of information.

1B.4 | Basics of Neurotransmission: Post-synaptic Responses

When an action potential (AP) moves down the axon, the signal reaches the axon terminal, depolarizing pre-synaptic voltage-gated calcium (Ca^{2+}) channels as described in detail by Purves et al., (2001b). Extracellular Ca^{2+} enters the axon terminal, increasing intracellular [Ca^{2+}]. This triggers a complex chain of biochemical reactions that ultimately lead to the exocytosis of docked synaptic vesicles. The synaptic vesicles containing chemical messengers, or neurotransmitters, are released into the synaptic cleft upon fusion with the axon terminal. The neurotransmitters diffuse across the synapse to the post-synaptic membrane. There, they come in contact with post-synaptic receptors.

Depending on the type of neurotransmitter emitted and receptors present, different ions will enter the cell. The influx of those ions causes changes in the membrane potential of the post-synaptic cell (Purves et al., 2001a). This results in post-synaptic potentials (PSP), which can be excitatory (EPSP) or inhibitory (IPSP). In contrast, electric post-synaptic currents (PSC) measure the ions flowing into the cell. The convention in electrophysiology names inward currents as excitatory post-synaptic currents (EPSC) and outward currents are referred to as inhibitory post-synaptic currents (IPSC). Following synaptic transmission, neurotransmitters are either degraded or reuptaken for future neurotransmission events (Purves et al., 2001c).

1B.5 | Basics of Neurotransmission: Pre-synaptic vesicular mechanisms

In order to transmit incoming stimuli, presynaptic cells must release vesicles containing neurotransmitters. There are 3 different vesicle pools: First, the readily releasable pool (RRP) is docked and ready for synaptic release and transmission (Guo et al., 2015). Second, the recycling pool is a transition group that either acts to refill the RRP or recycle the vesicular membranes. Third, the reserve pool provides the other pools with supply or proteins or can be used as a vesicle reservoir for the IP . When there is a large incoming stimulus, the presynaptic cell responds by releasing vesicles from the RRP, resulting in a large initial amplitude in the excitatory postsynaptic current (EPSC). This leaves the RRP depleted and unable to respond as quickly to further stimulation. However, if the presynaptic cell is able to modulate its vesicular release, where it releases more vesicles as more stimuli arrive, rather than all at the beginning (i.e. leading to facilitation), it will be able to deliver a stronger signal as the RRP is refilled (Guo et al., 2015). In other words, a high initial amplitude is correlated with a depressing synapse, while a high initial amplitude for a facilitating synapse. Meanwhile, release probability (RP) is a measure of the likelihood that vesicles will be released in response to a stimulus (Denker & Rizzoli, 2010). The lower the RP, the more likely the synapse is facilitating. Therefore, initial amplitude and RP are positively correlated to each other, and both are inversely correlated to facilitation (i.e. low amplitude and RP = more chances of facilitation).

1B.6 | Patch-Clamp Recordings

A common way to experimentally evaluate synaptic transmission is by using a recording method called the patch-clamp or "patching a neuron." The technique was developed by Sakmann and Neher in the 1970s to measure changes in membrane potential and currents of neurons (B Sakmann & Neher, 2003) Their method established the way for us to answer: *What happens inside a neuron? How do ion channels function in neurons?* Despite the novel techniques developed since then, patch-clamp is still widely used to understand neural mechanisms of transmission.

There are many types of patch-clamp recording configurations, but I will only describe whole-cell recordings in detail for the relevance of this project. Whole-cell recording is the most common way to evaluate post-synaptic responses to pre-synaptic transmission. To record the cell, a glass pipette with a thin tip is filled with an intracellular solution similar to the ionic composition inside a cell (Segev et al., 2016). A recording electrode is placed inside the recording pipette, immersed in the intracellular solution. Positive pressure is applied to the recording electrode and slowly lowered onto the region of interest. Once the cell is reached, confirmed by a "dimple" like shape, positive pressure is released. This creates negative pressure onto the cell and a seal between the cell and the recording electrode. With negative suction, the seal

breaks, forming a membrane patch where the cell makes direct contact with the recording electrode.

The two modes of whole-cell recording are voltage-clamp and current-clamp. Voltage-clamp was first developed by Hodgkin and Huxley on giant squid axons (Schwiening, 2012). They used the squid due to its large size and from their experiments developed the Hodgkin–Huxley model to explain the mechanisms of action potential propagation (Hodgkin & Huxley, 1952). In voltage-clamp mode, the cell is "clamped" and held constant at a certain membrane potential (e.g. -70mV). EPSCs and IPSCs are recorded in voltage-clamp mode. The recording is of the current that is required to be injected in order to maintain the cell at the clamped potential (Segev et al., 2016). Meanwhile, EPSPs and IPSPs are observed in current-clamp mode, where the current is fixed and the changes in membrane potential are recorded.

1B.7 | Short-Term Plasticity

Neurotransmission is a dynamic process. Each step can be modulated based on activity. This modulation in response to changes in activity is called synaptic plasticity (Citri & Malenka, 2008). Synaptic plasticity is usually divided into two timescales: short-term plasticity (STP; 10-100 milliseconds) and long-term plasticity (LTP; hours and days) (Andersen et al., 1966; Bear & Malenka, 1994; Bliss & Lomo, 1973; Malenka, 2003; Malenka & Bear, 2004; Nicoll, 2017). The mechanisms of short- and long- term plasticity have similar traits, but STP has mainly pre-synaptic mechanisms and LTP mostly post-synaptic (Volianskis et al., 2013). We will focus on discussing the mechanisms of short-term plasticity in this next section.

Short-term plasticity comes in two forms: short-term facilitation (STF) or short-term depression (STD). STF happens when synaptic response is larger after high frequency stimulation. This change in response is proposed to be important for the transfer for information and processing between neurons (Jackman & Regehr, 2017). To study the mechanism of facilitation, a pair of stimuli is used, called paired-pulse facilitation (Figure 3). Meanwhile, STD happens when given the same stimulation a smaller response happens. The mechanisms for STD is thought to be due to a decrease in the readily releasable pool of synaptic vesicles, thereby decreasing neurotransmitter release. However, then how does STF both use RRP to transmit signals and continue to release more to transmit even stronger signals? The mechanism for STF is then thought to be replenishing the RRP in some way.

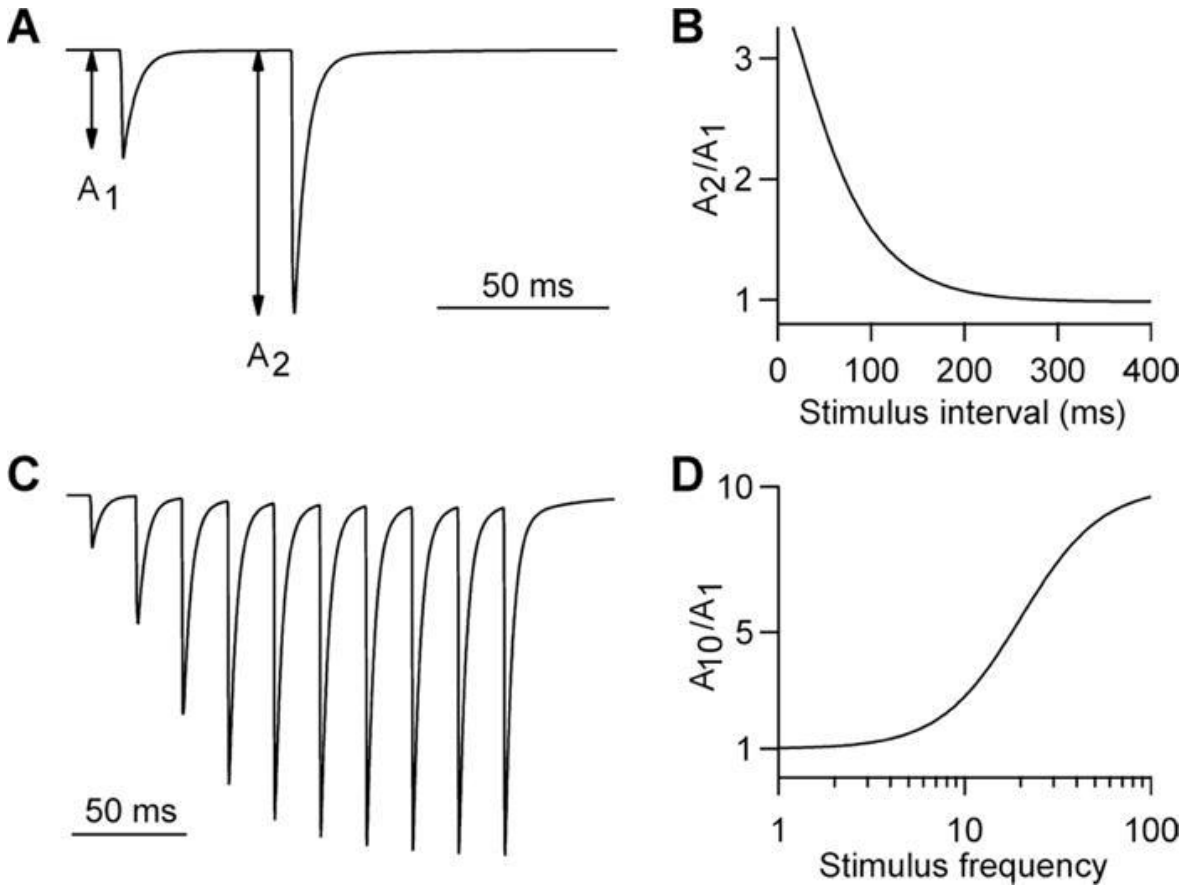

Figure 3 | (A) Evoked EPSC events by pair of stimulus with an inter-stimulus interval of 50ms. The paired-pulse ratio is used to measure facilitation **(B)** Typical change in paired-pulse ratio with increasing inter-stimulus intervals **(C)** 10 stimulus train of 50Hz leads to facilitation **(D)** Facilitation as a function of stimulus frequency (Jackman & Regehr, 2017).

1B.8 | Rate Coding

The basic, textbook definition of rate coding is that the propagation of signals in neurons is based on the frequency of the electrical activity down an axon and not the magnitude (Kandel & Schwartz, 2014). This is most apparent in the sensory system, where in the presence of sensory stimuli, neurons fire in different firing patterns. For example, the difference between holding a 5lbs or a 25lbs dumbbell, the heavier one will cause a motor neuron to fire faster compared to the lighter one. At the sensory level, the encoded information of firing activity is directly related to a sensory stimuli. In other words, the neural code can be directly decoded back to its sensory input. Whereas at the synaptic level, rate coding is a little bit more complex. What does the neural coding or changes in frequency mean in brain areas that are not receiving direct

inputs from the senses? This is a big question in the field of neural coding, in particular to information transfer in CA3 synapses, which will be the focus of Chapter 1 Part C.

Chapter 1

Part C | Hippocampal Circuits: CA3 Synapses and Dynamics

Introduction: Hippocampal Formation Circuit & Spatial Navigation

1C.1 | Hippocampus: Trisynaptic Loop

The discovery, naming, and history of the hippocampus was covered in Chapter 1A. In this section, we will evaluate the hippocampus at the circuit and synaptic level. We want to know *what are the neuronal circuits involved with memory? How do these neurons transmit information to generate memories?* We will introduce how the hippocampus is central for processing declarative memories, specifically encoding spatial information. Then we will look into how that fits within the greater brain network.

The hippocampus is a bilateral brain structure located in the medial temporal lobe, within the cerebral cortex. The densely packed principal cell layer and organised

projections make for easy visualisation of the hippocampus (Förster et al., 2006). With a microscope and patch-clamp rig, there are many options to study neurotransmission within the hippocampus. From a behavioural stand-point, the hippocampus is involved with contextual memory. The location of the hippocampus being not too deep, provides experimenters easy access for optogenetic, mini-microscope, and other behavioural manipulations. This gives experimenters the ability to examine questions at both the circuit and behavioural level. These anatomical properties make the hippocampus an ideal candidate to investigate all sorts of questions, ranging from neurotransmission to long-term decision making (Lüscher & Malenka, 2012; Miller et al., 2023). Since my work is on mossy fibre synapses, I will focus on introducing the cellular and circuit level properties of the hippocampus.

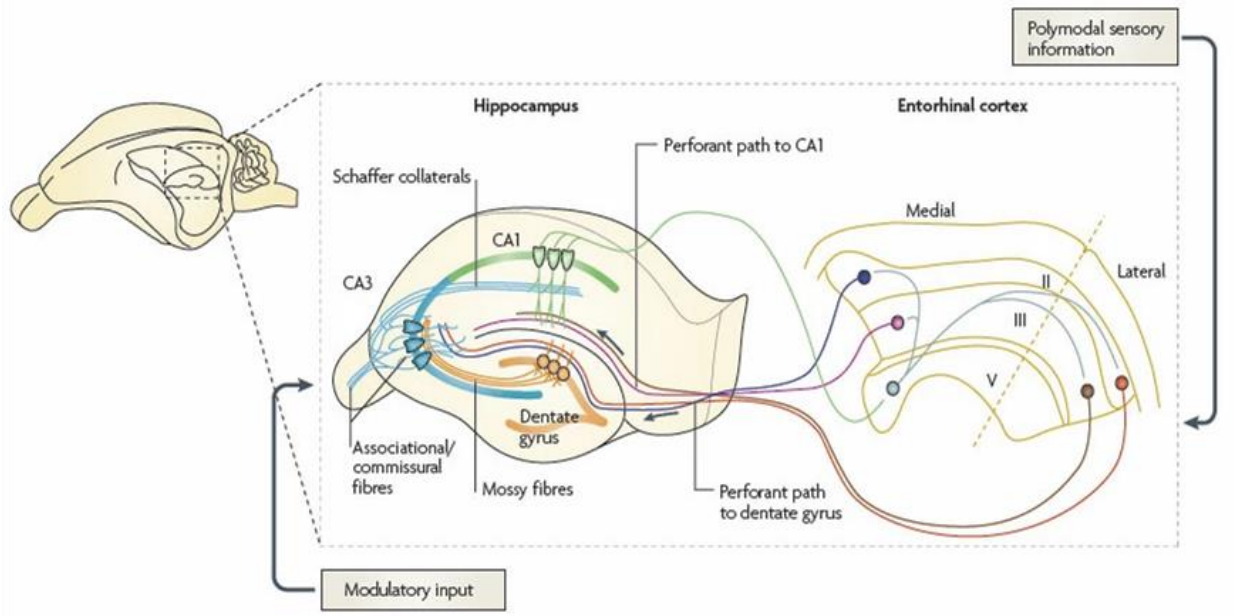

Figure 4 | Circuit diagram of the hippocampal formation from the perspective of a hippocampal slice and their connections between the layers of the entorhinal cortex (Neves et al., 2012).

Trisynaptic Loop | At the circuit level, the hippocampus forms the trisynaptic loop, connecting the dentate gyrus to the CA3-CA1 regions and subiculum (Figure 4, left). The first synapse of the trisynaptic loop receives inputs from layer II/III of the medial entorhinal cortex to the dentate gyrus of the hippocampus, forming the dentate perforant path (Neves et al., 2012). A parallel perforant path projects inputs from layer II/III of the lateral entorhinal cortex to the CA1 (Figure 4, right). Next, dentate granule cells send axon projections called mossy fibre axons (MFA) that terminate onto dendritic thorny excretions of CA3 pyramidal cells. MFAs will be discussed in more detail in Section 1C.3. Lastly, the CA3, via the schaffer collaterals, synapses onto CA1 pyramidal cells, which ultimately feeds back to layer V of the lateral entorhinal cortex (Figure 4, bottom). *What is the functional role of the trisynaptic circuit?*

1C.2 | Hippocampal Formation: Spatial Navigation

In Chapter 1A, we covered the discoveries of Milner and her team that demonstrated the hippocampus played a central role in formation and retention of new memories. However, those studies did not cover the underlying neuronal activity or neurotransmission mechanisms. There are ethical and technological limitations to answering those questions in humans, but model organisms are a great tool for researchers. Specifically, mice and primates were an ideal candidate because the hippocampus is well conserved across these species. The combination of behavioural paradigms and electrophysiology recording granted experimenters with target-specific manipulations to interrogate the underlying neuronal activity.

Place Cells | In the 1970s, English neuroscientists O'Keefe and Dostrovsky examined the behaviour of freely moving rats, while probing their hippocampus with extracellular electrodes (O'Keefe & Dostrovsky, 1971). Their experiments uncovered a more definite role of the hippocampus: distinct hippocampal cells (i.e., 'place units') would spike when the animal was in a specific area (i.e., 'place field') of the open-field arena (Figure 5). In another place field, a different place unit would fire. They called the units place cells. These preliminary results would later be formalised in O'Keefe's 1976 paper "Place units in the hippocampus of the freely moving rat (O'Keefe, 1976)." He proposed these cells as the neural correlates of the "Cognitive Map Theory" Tolman introduced in the late 40's (Tolman, 1948).

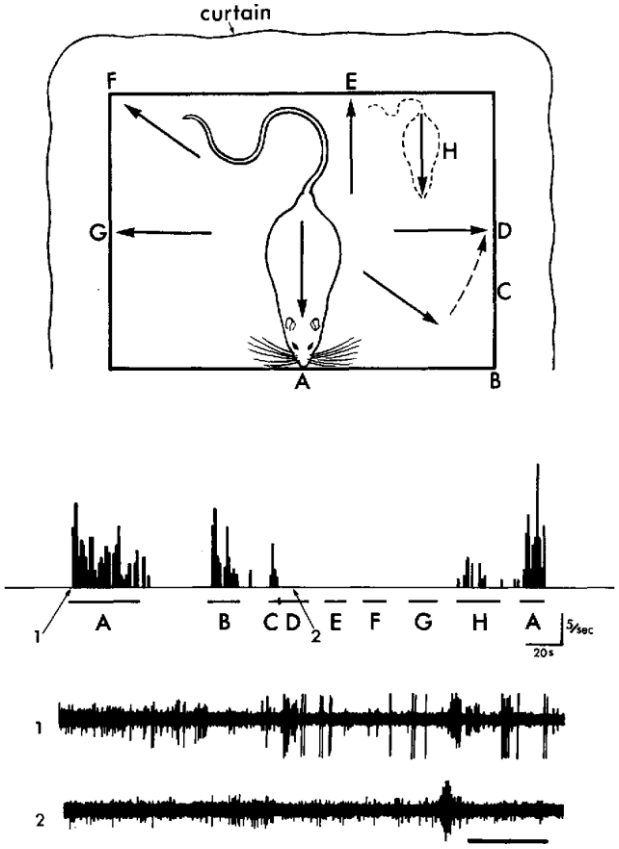

Figure 5 | Diagram illustrating the initial discovery of place cells. *Top:* A mouse in an open-field arena with each letter demonstrating a specific location. *Bottom:* The corresponding firing activity of each lettered location within the arena. This demonstrating that each individual location was encoded by a different neuron or place cell (O'Keefe & Dostrovsky, 1971).

Cognitive Map | In 1948, American psychologist Tolman coined the term 'the cognitive map' (Tolman, 1948). He proposed the theory to explain the brain processes required for

flexible and accurate wayfinding. For example, an animal escaping from a predator can either run a predetermined route to a known hideout, or scurry around searching for a safe space. The former is easier, but requires a mental map (Behrens et al., 2018). Tolman's cognitive map was a foundational theory, but it left researchers with the question: *How does the brain form a spatial map?*

Forming a mental map is a laborious and involved neural process. It involves collecting sensory information and integrating previous experiences to make real-time decisions. The underlying neural network is a complex system of storage, consolidation, and retrieval. As humans, we have developed tools (i.e. compass, map, GPS) to facilitate navigation and ease our reliance on mental representations. For animals, mental maps are imperative for survival. Spatial navigation is required to search for food, suitable mates, shelter, and evade predators with ease and efficiency (Clemenson et al., 2021). *What tools do animals use to navigate? How do animals gather sensory information to form cognitive maps?* Animals apply two main types of navigational methods, egocentric and allocentric. They use these methods to travel accurately from one place to another and to form cognitive maps. Egocentric navigation relies on the individual's relationship with respect to its environment (Figure 6, left).

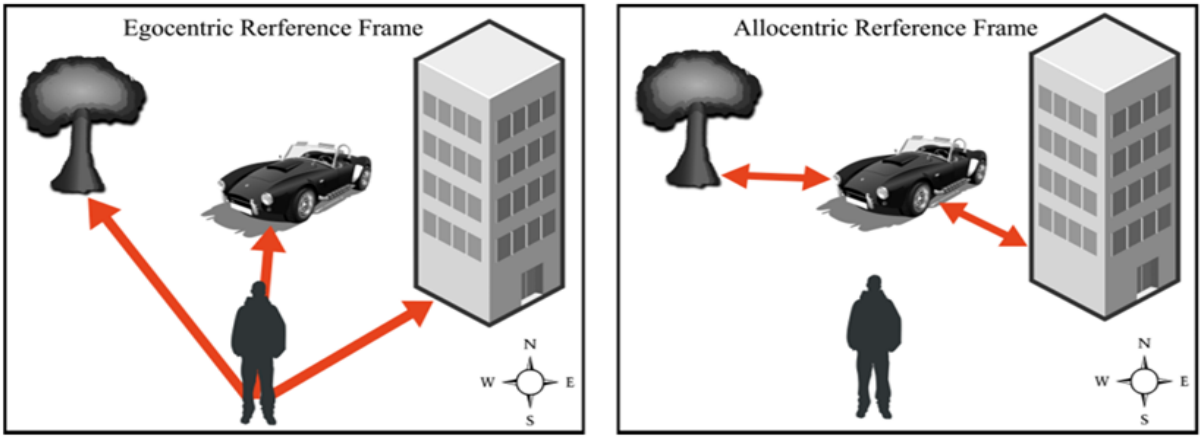

Figure 6 | Illustration of egocentric vs allocentric points of reference used for spatial navigation (Goeke, 2018).

The frame of reference is the individual. In other words, all external cues, such as landmarks and sensory inputs, are dependent on the position and orientation of the individual. Specialised senses, such as optic flow in bees or sonar in baths, and path integration are all examples of egocentric tools (Esch & Burns, 1995; McNaughton et al., 2006; Wittlinger et al., 2006, 2007; Wolf, 2011; Yamada et al., 2020). In contrast, allocentric navigation relates external cues to each other, independent of the individual (Figure 6, right). This means the point of reference is based on an 'object-to-object' relationship rather than 'object-to-self' (Clemenson et al., 2021). Both egocentric and

allocentric navigation are important for animals to adapt to changes in their environment in order to survive (Behrens et al., 2018; Bouchekioua et al., 2021).

Grid Cells | While navigating, animals also employ cognitive tools to explore. O'Keefe described the location-specific activity of place cells in the CA1. Place cells gather sensory information to encode for a physical representation of space. In contrast, Norwegian May-Britt Moser and Edvard Moser uncovered the entorhinal grid cells (Hafting et al., 2005). Grid cells fire in a particular pattern, similar to the shape of a hexagonal grid (Figure 7). Hence, 'grid' cells. As the animal moves around different environments, multiple activity fields are activated (Fyhn et al., 2007). This evidence suggested that grid cells produce a geometric representation of space, rather than a physical one like place cells (Moser et al., 2008).

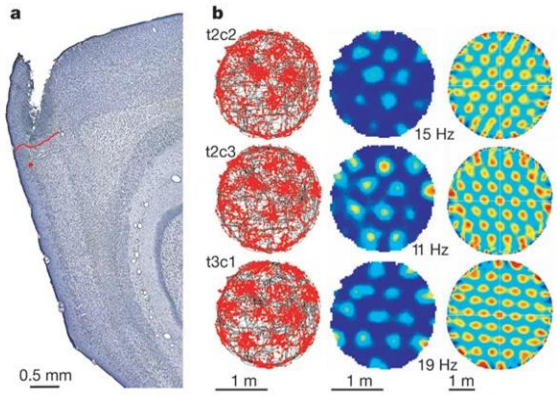

Figure 7 | a) Entorhinal cortex location of grid cell recordings. **b)** Visual representation of grid cells with their hexagonal firing patterns, in respect to heat maps and actual location (left column; Hafting et al. 2005).

Combined, CA1 place cells and entorhinal grid cells, connected the entorhinal cortex and the hippocampus to establish the hippocampal formation as the structure to study for spatial navigation (Muñoz-López, 2015; O'Keefe & Nadel, 1978). As a whole, the formation integrates sensory information required for forming spatial maps, with the main processing happening in the hippocampus (Davidson et al., 2009; Moser et al., 2017).

Do hippocampal neurons only represent space? A large portion of the literature covered up to this point has been focused on cognitive maps and navigation. These are specific processes of context-binding, dependent on the hippocampus (Yonelinas et al., 2019). There is evidence of more hippocampal-independent encoding that only requires the hippocampus for processing. Yet, the evidence suggests the hippocampus has many more functions such as replay, planning, predictions, decision-making and fear response (Buzsáki, 2015; Gillespie et al., 2021; Kjelstrup et al., 2002; Miller et al., 2023; Ólafsdóttir et al., 2018). From a memory perspective, the hippocampus is often implicated for encoding memories, but we often dismiss its role in forgetting memories or the granule cells as the centre for neurogenesis (Berdugo-Vega et al., 2020; Lazarov & Hollands, 2016; Richards & Frankland, 2017; Xu & Südhof, 2013).

Introduction: MFA and DG-CA3 network

1C.3 | DG-CA3 Network

The dentate gyrus to CA3 synapse (DG-CA3) is a critical component of the hippocampal formation involved with navigation, spatial learning and memory. As the first relay of the hippocampal loop, the dentate gyrus (DG) receives and integrates entorhinal cortex inputs and delivers them to the hippocampal CA3 neurons (Figure 8A). The cortical information is transmitted by way of dense firing patterns, which must be converted to hippocampal firing before CA3 processing (Diamantaki et al., 2016). The DG granule cells perform this conversion by transforming densely coded signals (short bursts) into sparsely coded information (bursts with long interburst intervals). In short, the DG granule cells act as a code-switch centre between cortical regions and the HPC (Krueppel et al., 2011). This first synapse of the trisynaptic loop plays an important role in integrating cortical signals for hippocampal processing (Figure 8B).

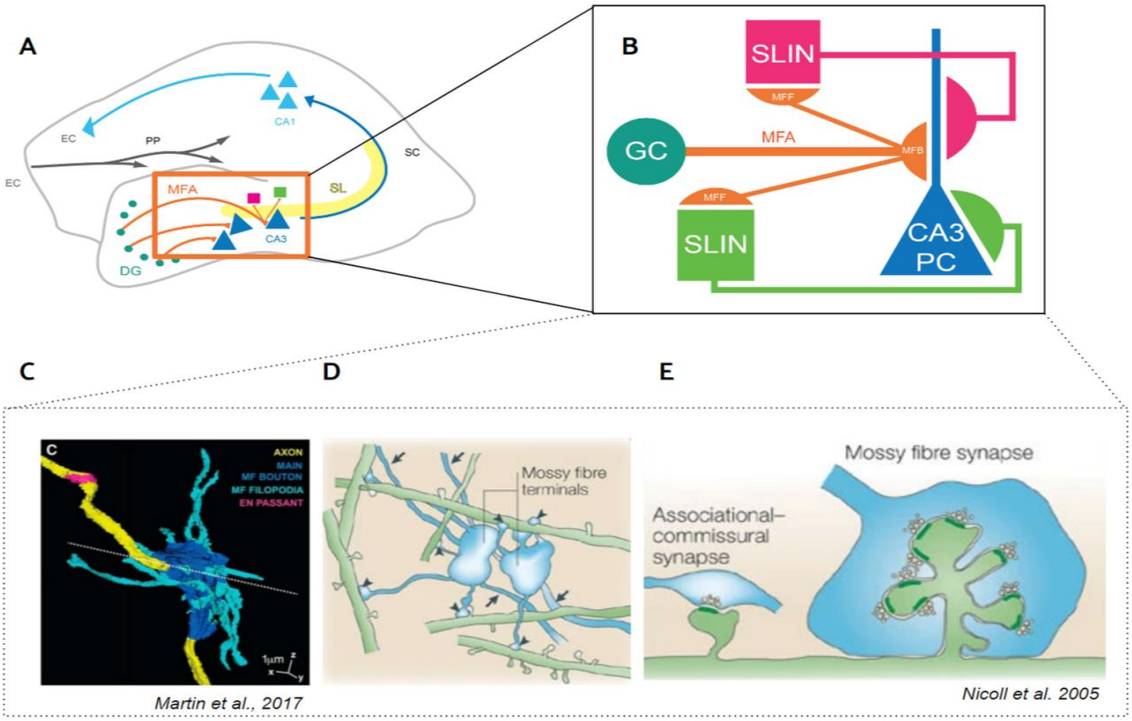

Figure 8 | Trisynaptic loop, CA3 circuits, and mossy fibre synapses | **(A)** Illustration of mouse hippocampal slice, the view of the trisynaptic loop. **(B)** Larger magnification of the CA3 area with the main synaptic players. **(C)** 3D reconstruction of the CA3 terminals with main players coloured (Martin et al., 2017). **(D)** Depiction of mossy fibre synapses wrapping around CA3 dendrites. **(E)** Large mossy fibre terminal types (Nicoll & Schmitz, 2005).

Mossy Fibre Axons | To understand how the DG and CA3 communicate, we must first discuss the unique morphology of mossy fibres (Figure 8C-E). DG granule cells form mossy fibre axons (MFA) when connecting to CA3 pyramidal cells. MFAs play a critical role in processing information. They have 3 specialised forms of synaptic morphology to process information: **1)** mossy fibre boutons (MFB), **2)** mossy fibre filopodia (MFF), **3)** en passant mossy fibres (Acsády et al., 1998). MFBs are the largest MFAs and have 20-40 release sites. They directly terminate onto specialised dendritic spines of CA3 pyramidal cells, called CA3 thorny excursions (TEs) (Martin et al., 2017). Meanwhile, MFF extends from MFBs with single release sites (Figure 8B, C). They connect onto Gamma-aminobutyric acid (GABA) expressing interneurons (IN), located mainly in the stratum lucidum layer of the CA3 (Figure 8A, B) (Acsády et al., 1998)). These GABAergic stratum lucidum interneurons (SLINs) provide inhibitory modulation to downstream CA3 pyramidal cells (Pelkey et al., 2005). Whereas, en passant mossy fibres with single release sites terminate along CA3 pyramidal dendrites. Together, these varied synapses between MFAs and CA3 pyramidal cells produce an excitatory and local feed-forward inhibition within the DG-CA3 network (Torborg et al., 2010).

There are 4 main types of synapses within the dentate gyrus - CA3 (DG-CA3) network (Acsády et al., 1998): **1)** Entorhinal cortex (EC) to DG granule cells (hereafter referred to as EC-DG), **2)** DG granule cells to CA3 pyramidal cells via mossy fibre boutons (MFBs; hereafter referred to as MFB-CA3PC; Chamberland et al., 2018) **3)** DG granule cells to CA3 stratum lucidum interneurons via mossy fibre filopodia (MFFs; hereafter referred to as MFF-SLIN; Acsády et al., 1998), **4)** CA3 stratum lucidum interneurons to CA3 pyramidal cells (Figure 8B; Torborg et al., 2010). The MFAs are the central highway of the DG-CA3 network and are therefore ideally positioned to gate local information transfer. MFAs carry out this gating function by utilising the previously discussed specialised forms of MFA synapses (Chamberland et al., 2018).

1C.4 | Coding Strategies in the DG-CA3 Network

1C.4.1 | EC-DG Coding

Research from other labs have studied the EC-DG and EC-DG and stratum lucidum interneuron (SLIN)-CA3 connections in detail (Krueppel et al., 2011; Rebola et al., 2017; Torborg et al., 2010). They showed mechanisms of dendritic signal integration was important for transmission in CA3 interneurons and sparse coding for EC-DG networks. However, little is known about how the MFB-CA3 pyramidal cell (CA3PC) and MFF-SLIN encode information.

1C.4.2 | MFB-CA3 Coding Strategies: AP Counting

Previous published work from our lab has shown MFBs employ a unique coding strategy when transferring information to CA3, they do so by using a 'counting logic' (Chamberland et al., 2018). They evaluated MFB-CA3PC synapses with the following stimulation protocol: **A:** 6x20Hz, **B:** 6x100Hz, **C1:** 5x20Hz + 1x100Hz and **C2:** 5x100Hz + 1x20Hz. Each protocol totalled 6 stimulations. Protocols A and B differ in frequency (20Hz vs 100Hz). Meanwhile, protocols C1 and C2 averaged 120Hz, with a combination of low (20Hz) and high (100Hz) frequencies. Chamberland et al, 2018, discovered that the postsynaptic CA3 PCs would consistently fire after the 6th presynaptic GC action potential (AP). Although the number of incoming stimuli mattered, the PC largely disregarded the frequency of the first 4 stimuli (burst frequency), with exception of the last 2 spikes (instantaneous frequency; Figure 9; Chamberland et al., 2018). In other words, MFB tracts prescribed a condition based on counting to 6 before PCs can fire an AP, but neglected the time difference between stimuli. This coding method at the MFB-PC synapse was named 'AP Counting.'

The type of 'counting logic' had never before been described. This novel way for MFB to gate information transfer to the CA3 begged the question, if this counting approach is observed at one type of MFA synapses, *can it also be applied to the other types?* Namely, do MFF-SLIN synapses also apply AP Counting? *If not, what are the coding mechanisms of MFF-SLIN synapses?*

1C.4.3 | MFF-SLIN Coding Strategies: Unpublished Results

There is no published work on coding strategies in MFF-SLIN synapses. Our lab however has unpublished data using the same stimulation protocol from 'AP Counting' that identified two possible MFF-SLIN coding strategies in rats (Chamberland et al., 2018). The two strategies differed in various synaptic properties: initial amplitude, sustained release, and morphology. Due to previous publications from the lab, we suspect these two strategies are employed by two different subpopulations of SLIN cells, with different molecular compositions. We named the two subpopulations and their respective coding strategies, SLIN subpopulation 1 (SLIN1) and SLIN subpopulation 2 (SLIN2). SLIN1 demonstrated mechanisms similar to rate coding, while SLIN2 was frequency insensitive. Since these experiments were performed in rats, the work performed within this thesis used mice in order to validate whether these differences in coding strategies were similar between rats and mice. My work was performed in mice to enable future studies to use transgenic mice to explore differences in molecular mechanisms of MFF-SLIN synapses.

Chapter 2

The Mechanisms and Molecular Dynamics of MFF-SLIN Coding Strategies

2.1 | MSc Thesis Objective and Hypothesis

The objective of this thesis was to decipher the diversity of coding methods utilised at local networks of the DG-CA3 system, whether it was counting, responding to frequency, or applying another method. We specifically wanted to examine MFF-SLIN synapses, in mice, within the CA3 network.

To elucidate the methods of synaptic transmission at MFF-SLIN, whether they applied 'AP Counting' like MFB-CA3PC synapses, or used other mechanisms. CA3 synapses were evaluated using the 4 stimulation protocols shown in Figure 9C. The protocols kept the same total number of stimuli, with variations between low (20Hz) and high (100Hz) frequency and a combination of the two. Based on previous rat data, we expected to find more than one MFF-SLIN coding strategy.

Due to the small sample of SLIN cells with GC origins and many cells with CA3 origins, we added a sub-objective for this thesis. In addition to evaluating MFF-SLIN coding strategies, we also examined the CA3-SLIN coding strategies.

2.2 | Results

2.2.1 | Results from Selection Criteria Filtering

In total, I investigated 267 cells "magic cut" hippocampal slices (Figure 9A) from 100 male mice and 19 female mice. Given the experimental challenges of recording MFA inputs, it was expected that not all cells would demonstrate sufficient responses. From the 267 cells, 55 cells (female n = 2; male n = 31) responded to our stimulation protocol and were analysed and evaluated based on our selection criteria (see Section 2.5.5 | Data Selection Criteria for more details). The cells that met none of the selection criteria were removed (n = 16). Most of the cells that did not meet any section criteria were polysynaptic with large access resistance (Ra), beyond our threshold of 30MΩ. Out of the remaining 39 cells, 14 cells demonstrated clean monosynaptic traces, but did not meet all of our selection criteria. For example, a cell with a clean monosynaptic response that was within a holding range of -50pA to 50pA, with an Ra that was inconsistent across the protocols or that fluctuated beyond the +/- 20% range of our criteria (most were at approximately 25%). Another occurrence was if only one protocol had an Ra beyond the acceptable range, but all the other protocols remained within the range. Thus in the end, a total of 25 cells (3 cells from 2 female mice and 22 cells from 16 male mice) met all of the selection criteria and were included in our study to ensure that we were only using and comparing the highest quality electrophysiology data.

2.2.2 | CA3 SLIN Recordings: MFF-SLIN vs CA3-SLIN

We compared the responses of the 25 cells that passed our selection criteria to the stimulation protocols: **A:** 6x20Hz, **B:** 6x100Hz, **C1:** 5x20Hz + 1x100Hz and **C2:** 5x100Hz + 1x20Hz (Figure 9C). On the population level, these cells demonstrated a variety of short-term dynamics. These cells demonstrated a facilitating evoked EPSC response across all protocols. Between protocols A and C1, the two protocols with 5 pulses of 20Hz trains showed a more linear response from peak 1 to peak 6 (Figure 9I, 9K). Meanwhile, the 100Hz protocols B and C2, exhibited a "hill-shaped" response (Figure 9J, 9L). When comparing the 6th EPSC amplitude of the protocols with 20Hz and 100Hz, they did not show similar short-term plasticity. However, the results from Figure 9 did not distinguish whether the inputs have origins from the DG axons or CA3 collaterals.

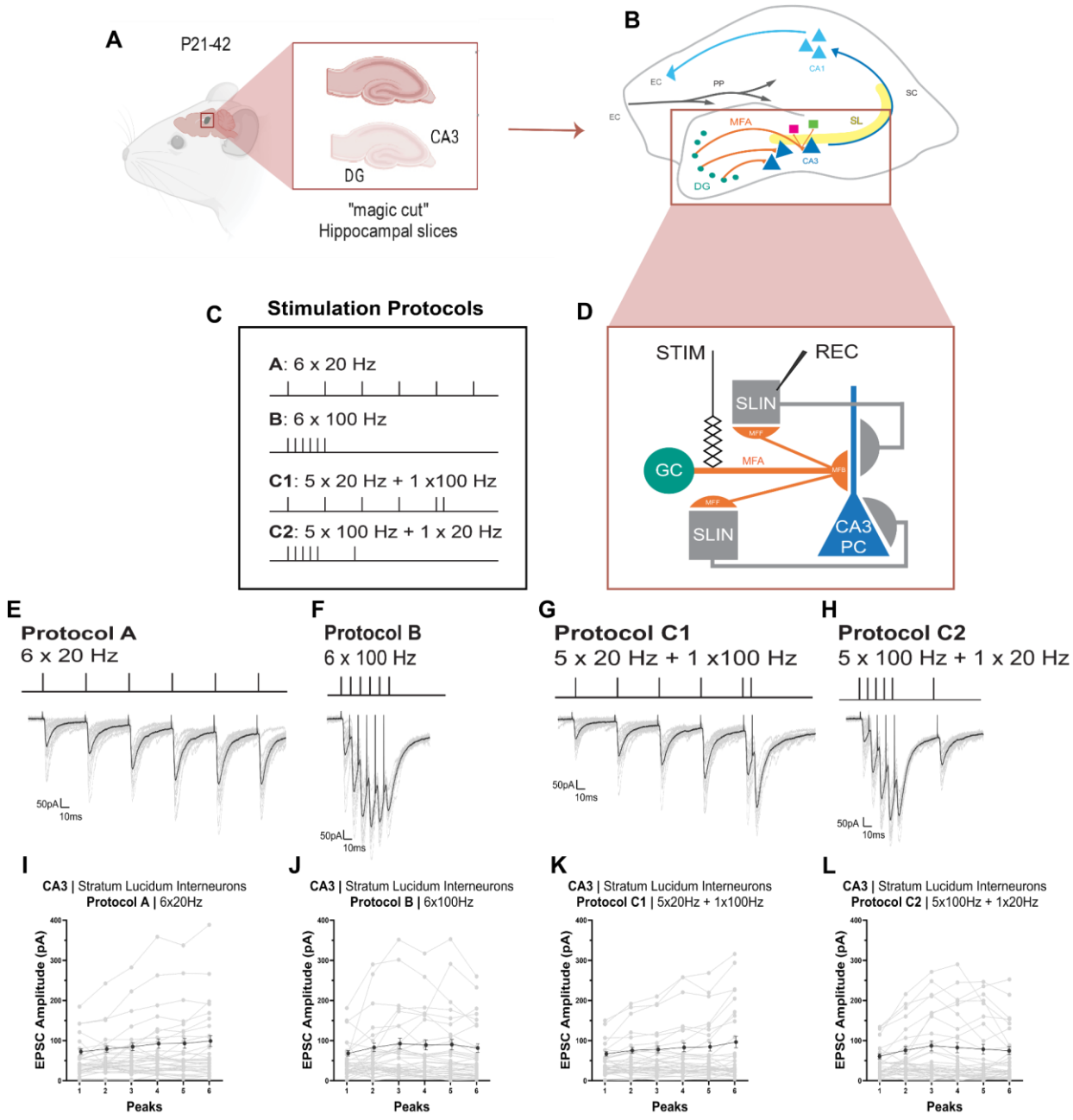

Figure 9 | Experimental Setup and SLIN Response to Stimulation Protocols A, B, C1, and C2 | (A) Illustration of "magic cut" hippocampal slices, extracted from a P21-42 mouse brain. **(B)** Hippocampal slice with the trisynaptic circuit. The stratum lucidum layer (SL) is highlighted in yellow, where the stratum lucidum interneurons (SLIN) are found. **(C)** Graphic of Stimulation Protocols: A, B, C1, and C2. **(D)** Schematic of CA3 cells, axons, and microcircuit. The stimulating electrode is on the mossy fibre axons (orange) and the recording electrode on CA3 SLIN (grey). **(E-H) Top:** graphical representation of stimulation protocols A, B, C1, and C2 **Bottom:** EPSC response traces of a single exemplary cell to the stimulation protocols. Lighter shades are individual sweeps with the darker trace as the average of 20 sweeps. **(I-L)** Corresponding EPSC amplitude response of each peak to protocols A,B, C1, and C2.

Individual cells are in the lighter shade with the mean + s.e.m. in the darker colour. **(A-L: Alphabetically-ordered Abbreviations):** *Cornu Ammonis* 1 (CA1), *Cornu Ammonis* 3 (CA3), CA3 pyramidal cell (CA3 PC), dentate gyrus (DG), entorhinal cortex (EC), excitatory postsynaptic currents (EPSC), granule cells (gc), mossy fibre axons (MFA), mossy fibre bouton (MFB), mossy fibre filopodia (MFF), perforant path (PP), recording electrode (REC), schaffer collaterals (SC), stratum lucidum interneurons (SLIN), stimulating electrode (STIM), stratum lucidum layer (SL).

We applied (2S,2′R,3′R)-2-(2′,3′-dicarboxycyclopropyl)glycine (DCG-IV) after the experimental protocols to confirm DG inputs (Figure 10A). DCG-IV is a selective Group 2 metabotropic glutamate receptor ($mGluR_2$ and $mGluR_3$) agonist (reference needed). Filtering the 25 cells based on their pharmacological response to DCG-IV, allowed us to selectively examine the transmission of MFF-SLIN compared to CA3-SLIN. Ten of the 25 cells were removed due to their lack of stable recording during DCG-IV application. From the remaining 15 cells that had DCG-IV recordings, in the presence of DCG-IV, EPSC transmission of SLIN cells with MFF origins were depressed (Figure 10B - orange trace), while cells with CA3 inputs were not depressed (Figure 10C - orange trace). Specifically, 12 of the 15 cells were insensitive to DCG-IV (Δ eEPSC < -49%) with only 3 of the 15 cells sensitive to DCG-IV (Δ eEPSC ≥-49%).

For the 12 DCG-IV insensitive cells, 2,3-dioxo-6-nitro-7-sulfamoyl-benzo[f]quinoxaline (NBQX), a competitive antagonist was applied to verify AMPAR-mediated responses (Figure 10B - purple trace). Lastly, the cells that responded to neither DCG-IV nor NBQX, had their membrane voltage increased by increments of +5mV until the EPSC reached the reversal potential of the cell. Collectively, these DCG-IV insensitive cells were grouped together as CA3-SLIN, regardless of their response to NBQX (Figure 10A, 10C). Therefore, based on DCG-IV sensitivity and for the future analysis below, the dataset of 15 cells with DCG-IV recordings were separated based on their input origins: GC inputs (n = 3) and CA3 inputs (n=12). The 12 cells with CA3 inputs (10 male mice and 2 female mice) and the 3 cells with GC inputs (1 female mouse and 2 male mice), were compared for Figure 10 and 11. The 3 cells with GC inputs are the cells with MFF-SLIN synapses, the main subjects of this study.

A

TABLE 1A | SLIN Recordings	# Cells	Fig #
All WT cells that met all the selection criteria	25	1
Table 1B | SLIN Input Types	**# Cells**	**Fig #**
Cells Removed: No DCG-IV Data	10	2
GC Inputs: >49% DCG-IV ESPC reduction	3	2
CA3 Inputs: <49% DCG-IV ESPC reduction	12	2

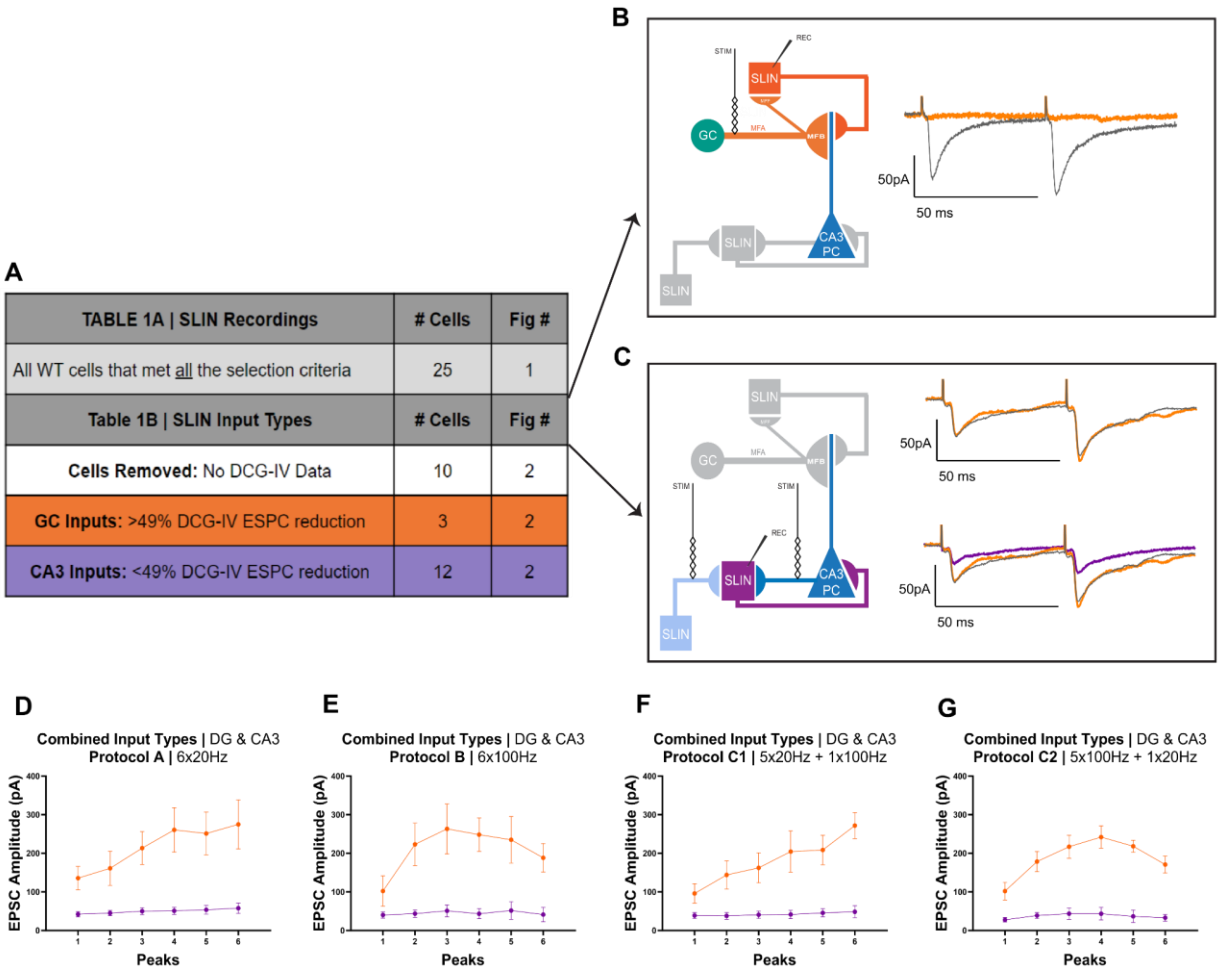

Figure 10 | SLIN: GC vs CA3 Inputs | (A) Table 1A: Total number of cells that met selection criteria. **Table 1B:** sorting of all cells from Table 1A based on input types or lack of pharmacological evidence. **(B)** Recording of CA3 SLIN with GC axon stimulation; CA3 stimulation is greyed out. **Left:** circuit diagram when stimulating MFA input types. **Right:** EPSC response trace to 50m pair-pulse stimulation of a single cell: DCG-IV baseline (grey), reduction in response to pharmacological application of DCG-IV (orange). **(C)** Recording of CA3 SLIN with CA3 stimulation; GC axon stimulation is greyed out. **Left:** circuit diagram when stimulating from CA3 input types - other SLINs or CA3 PCs. **Right:** EPSC response trace to 50m pair-pulse stimulation of a single cell: DCG-IV baseline (grey), reduction in response to pharmacological application of DCG-IV (orange), NBQX (purple). **(D-G)** Mean + s.e.m. EPSC amplitude response of each peak to protocols A,B, C1, and C2. GC inputs from n = 3 cells (orange), CA3 inputs from n = 12 cells (purple). **(A-G: Alphabetically-ordered Abbreviations):** *Cornu Ammonis* 3 (CA3), CA3 pyramidal cell (CA3 PC), (2S,2'R,3'R)-2-(2',3'-Dicarboxycyclopropyl)glycine (DCG-IV), dentate gyrus (DG), excitatory postsynaptic currents (EPSC), granule cells (gc), mossy fibre axons (MFA), mossy fibre bouton (MFB), mossy fibre filopodia (MFF), (2,3-dioxo-6-nitro-7-sulfamoyl-benzo[f]quinoxaline) (NBQX), perforant path (PP), recording electrode (REC), schaffer collaterals (SC), stimulating electrode (STIM), stratum lucidum layer (SL), stratum lucidum interneurons (SLIN), wild-type (WT).

Are MFF-SLIN and CA3-SLIN different? When comparing the response dynamics between cells with DG and CA3 inputs, we observed a marked difference in their mechanisms of short-term plasticity. The mean EPSC amplitudes of MFF-SLIN is overall stronger than CA3-SLIN synapses (Figure 10D-G). Similarly, to the combined input types, MFF-SLIN strongly demonstrated a short-term facilitation mechanism with a linear pattern for protocols A and C1, with protocols B and C2 with the more "hump-shaped" trend (Figure 10A, 10C; 10B, 10D). CA3-SLIN synapses also follow a similar general shape, with peaks 3 and 4 a bit stronger than the remaining, but not enough separation to be classified as a distinct method of facilitation.

What are the MFF-SLIN coding strategies? To further investigate what coding mechanism CA3 interneurons employ we analysed the 6th EPSC amplitude to the 1st. We then normalised their response to protocol A. First we compared the normalised protocols to each other, or coding strategies, within and between input types. We found the response dynamics of MFF-SLIN synapses was less variant than CA3-SLIN synapses (Figure 11A, 11J). Visually, both input types can be sub-categorised into sub-populations based on their response dynamics. The Ca3-SLIN sub-populations were more pronounced than the ones found at MFF-SLIN synapses (Figure 11A, 11J). In contrast, MFF-SLIN coding mechanisms had similar responses, but were less distinct (Figure 11A). Second, we compared the traces between input types. MFF-SLIN exhibited a notably stronger trace than CA3-SLIN, clearly showcased by the quantitative data in Figure 11 B-E.

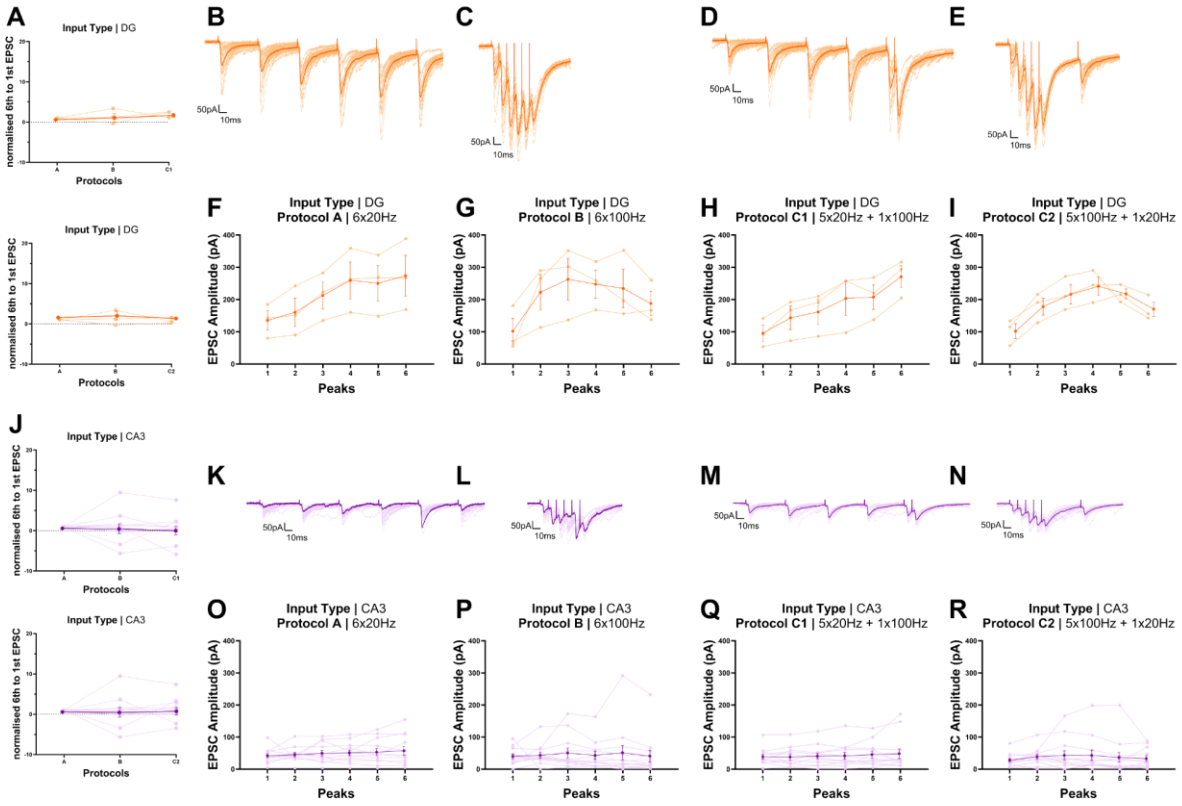

Figure 11 | Different responses of SLIN cells to stimulation protocols dependent on GC or CA3 inputs | (A) Normalised response of GC inputs from n = 3 cells (orange). **Top:** comparison between protocols A, B, and C1. **Bottom:** comparison between protocols A, B, and C2. **(B-E)** EPSC trace of an individual cell in response to CA3 stimulation of protocols A, B, C1, and C2 (orange). The lighter shade of orange are individual sweeps with the darker shade being the mean of 20 sweeps. **(F-I)** EPSC amplitude of GC inputs from n = 3 cells (orange). Lighter shades are individual cells with the mean + s.e.m. in the darker orange. **(J)** Normalised response of CA3 inputs from n = 12 cells (purple). **Top:** comparison between protocols A, B, and C1. **Bottom:** comparison between protocols A, B, and C2. **(K-N)** EPSC trace of an individual cell in response to CA3 stimulation of protocols A, B, C1, and C2 (purple). The lighter shade of purple are individual sweeps with the darker shade being the mean of 20 sweeps. **(O-R)** EPSC amplitude of CA3 inputs from n = 12 cells (purple). Lighter shades are individual cells with the mean + s.e.m. in the darker purple. **(A-R Alphabetically-ordered Abbreviations):** *Cornu Ammonis* 3 (CA3), excitatory postsynaptic currents (EPSC), granule cells (gc), stratum lucidum interneurons (SLIN).

Third, we compared the short-term plasticity of each input type. The data in Figure 10, led us to establish that the MFF-SLIN versus CA3-SLIN synapses had differences in short-term plasticity. This subsequent analysis of the same dataset enabled us to begin to demonstrate the underlying synaptic mechanisms that generate the differences observed in short-term plasticity at these two synapses. This analysis provided an overview of the method of synaptic transmission between the 1st and 6th EPSC of each

given protocol. We found that although MFF-SLIN synapses have a stronger facilitation, the variance between cells is more spread out than CA3-SLIN (Figure 11F-I; 11O-R). Both input types still exhibit a linear fashion of plasticity in protocols A and C1 and “hill-shaped” for protocols B and C2, but CA3-SLIN cells were remarkably weaker. Thus overall, these data suggest that both MFF-CLIN and CA3-SLIN synapses follow similar global trends of frequency-dependent plasticity, but with different strengths and variance based on their synaptic origin.

2.2.3 | MFF-SLIN Coding Strategies

What are the MFF-SLIN coding strategies? The synaptic transmission of MFF-SLIN synapses were be separated and summarised into 3 coding strategies and subpopulations: 1) SLIN subpopulation 1 (SLIN1): Traditional Rate Coding (n =1; male mouse), 2) SLIN subpopulation 2 (SLIN2): Frequency Insensitive (n = 1; male mouse), 3) SLIN subpopulation 3 (SLIN3): Frequency Dependent (n = 1; female mouse; Figure 12A-C). These coding strategies were also divided into *However, how are these mechanisms different?* Despite the small sample size, evaluation of the intrinsic properties from each coding strategy allowed us to uncover potentially distinct responses in each group. The cell categorised as Traditional Rate Coding (red exhibited more noticeably stronger initial EPSC amplitudes and slower kinetics than the other two subpopulations (Figure 12E-H; red). The cell in the Frequency Dependent (blue) group had weaker initial and final EPSC amplitudes, but demonstrated similar kinetics with the cell from the Frequency Insensitive group (Figure 12E-H; blue).

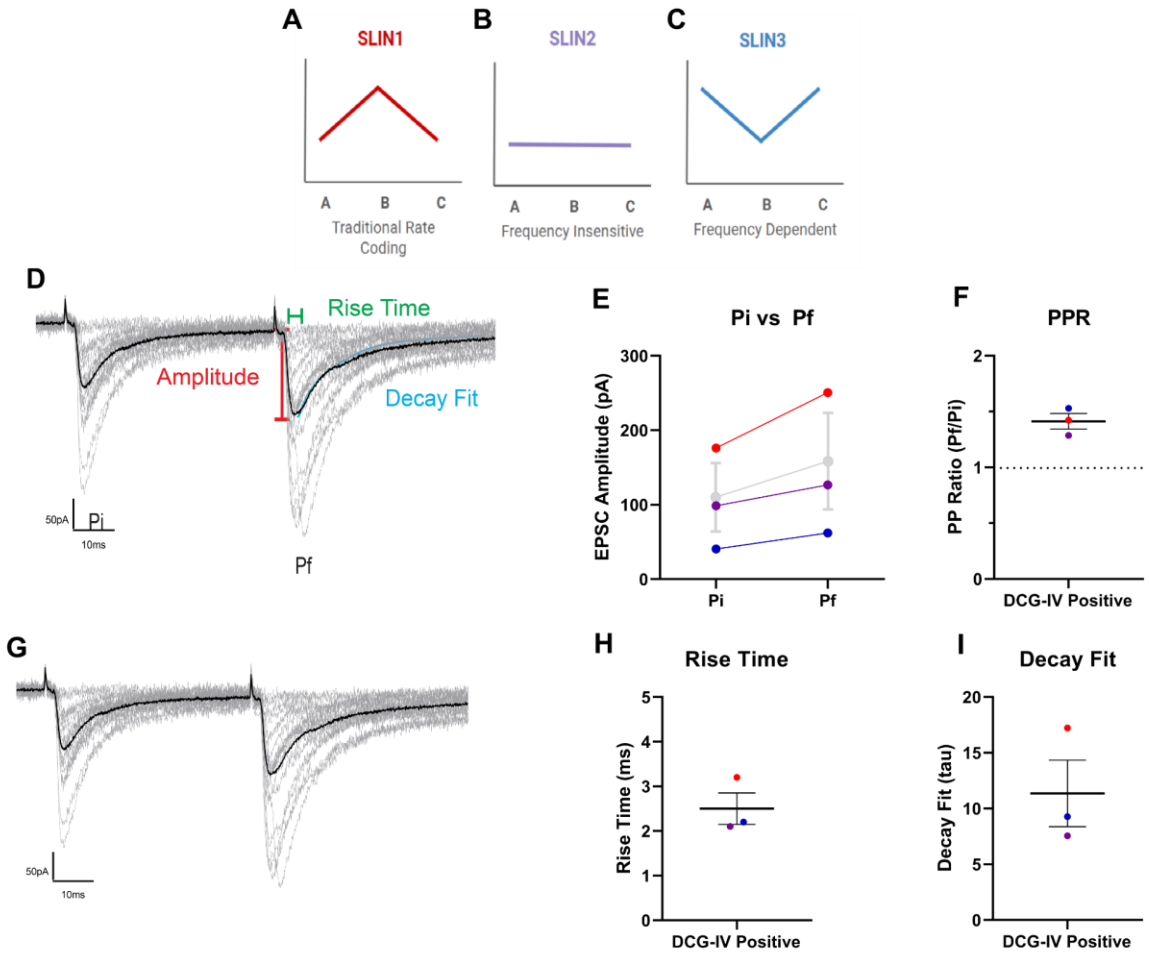

Figure 12 | Intrinsic Properties SLIN with MFF Inputs |
This data from this figure are the same 3 MFF-SLIN cells that were shown in Figure 11 A-I. The intrinsic properties were extracted from the paired-pulse ratio data from each MFF-SLIN subpopulation, grouped by coding strategies as shown in A-C. **(A-C)** 3 MFF-SLIN sub-populations grouped by coding strategies, which are based on their normalised responses to stimulation protocols A, B, C1, and C2. This sub-figure is an animated version of the data from Figure 11A **SLIN1:** traditional rate coding (red; n=1); **SLIN2:** frequency insensitive coding (purple; n=1). **SLIN3:** reverse rate coding (blue; n=1). **(D)** Schematic of quantitative data extracted from 50ms pair-pulse recording. Example trace from single cell with the darker shade being the average of 20 sweeps of lighter shade individual traces. **(E)** Comparison between Pi and Pf amplitudes. **(F)** PPR response between SLIN sub-populations. **(G)** Rise time of MFF-SLIN sub-populations. **(H)** Decay fit distribution. **(A-H: Alphabetically-ordered Abbreviations):** (2S,2'R,3'R)-2-(2',3'-Dicarboxycyclopropyl)glycine (DCG-IV), excitatory postsynaptic currents (EPSC), initial peak (Pi), final peak (Pf), pair-pulse ratio (PPR), stratum lucidum interneuron sub-population 1, 2, 3 (SLIN1,2,3).

2.3 | Discussion

2.3.1 | Target Specific Coding Mechanisms

This work took an exploratory approach to investigate whether MFF-SLIN synapses apply similar or different coding strategies from MFB-CA3PC synapses. The findings suggest that MFF-SLIN synapses use different mechanisms from MFB-CA3PC synapses within the limited sample sizes examined. When evaluating the short-term plasticity of MFF-SLIN, our data provides preliminary data to suggest varied and distinct methods of transmission. These variations could be summarised into 3 groups of SLIN cells with 3 types of coding strategies: 1) SLIN1: Traditional Rate Coding, 2) SLIN2: Frequency Insensitive, 3) SLIN3: Frequency Dependent.

Strategy 1 was named "Traditional Rate Coding" because the response type is similar to the basic principle of neuron rate coding (Kandel & Schwartz, 2014), where information is encoded and transmitted by neurons through the frequency or rate of action potentials (spikes) they generate over time (Figure 12A, Left). Traditional rate coding is a simple but effective way to represent information in neural systems. It is based on the idea that the intensity or strength of a stimulus is encoded by the firing rate of neurons, with higher rates corresponding to stronger stimuli. This activity is due to the "all or nothing principle" of action potential firing, where magnitude of the stimuli or the number of stimuli are not regarded.

Strategy 3 is similar to Strategy 1, but the relative intensity of the transmission is less potent and not more for protocol B (Figure 12C, Right). In contrast, the physiological responses of Strategy 2, across all protocols, did not vary with changes in the frequency of the stimulation pattern (Figure 12A, Centre). This strategy does not discriminate between frequency, nor the number of stimuli, which might indicate more general and flexible processing of information. In short, when SLINs cells in the CA3 were given the same pre-synaptic stimulation, the post-synaptic cell exhibited 3 different responses. Thus, these early findings suggest that transmission at mossy fibre axons are target specific.

2.3.2 | Cell-type Specific Coding Mechanism

A natural follow-up question to this data is *How are these different coding strategies generated? How are target-specific mechanisms determined? What happens at the synapses for there to be different coding mechanisms?* There are many approaches to address this question, I will focus on two main approaches in detail here. The first is by evaluating the molecular differences of synaptic transmission at MFF-SLIN synapses. The second is by evaluating the function of different interneuron subtypes in relation to the various coding strategies.

Molecular Composition of MFF-SLIN Synapses | Synapses are composed of 3 main compartments: presynaptic terminal, synaptic cleft, and postsynaptic terminal. Each compartment has individual players, contributing to the role of the compartment. Together, these players contribute to the overall dynamic process of synaptic transmission. *However, which of these elements are involved with distinguishing MFF-SLIN coding strategies? What differences in the composition of these synaptic elements could be the explaining factor of varied coding strategies? In short, are MFF-SLIN synapses built differently? If so, how?*

One synaptic player that has been identified to play a role in varying synaptic transmission is the protein, extracellular-leucine-rich repeat fibronectin domain 1 (Elfn1; Dunn et al., 2018; Stachniak et al., 2019; Sylwestrak & Ghosh, 2012; Tomioka et al., 2014). Elfn1 is a cell adhesion molecule expressed in the brain that is involved with synapse formation and function (Dunn et al., 2018). It has been implicated in playing a role in regulating synaptic plasticity, essential for information processing in terms of learning and memory (Sylwestrak & Ghosh, 2012). More specifically, Elfn1 has the potential to influence interneuron short-term plasticity by 1) Modulating presynaptic release probability 2) Interactions with synaptic adhesion mechanisms 3) Involvement with calcium dynamics. In 2012, Sylwestrak & Gosh demonstrated that Elfn was an active participant in CA1 pyramidal cell - interneuron (IN) facilitation. Their findings showed that inhibiting Elfn1 lowered the release probability (RP) in one subtype of CA1 interneurons (Parvalbumin; PV), while increasing RP in another subtype (Oriens-lacunosum moleculare; OLM). Given Elfn1 has been shown to affect RP between CA1 pyramidal cells and CA1 interneurons, this raises the question if Elfn1 could be involved in producing the different MFF-SLIN coding strategies. These questions could be tested using Elfn1 knockout (KO) mice in future studies.

In addition to Elfn1, mGluR7 and the α-amino-3-hydroxy-5-methyl-4-isoxazolepropionic acid receptors (AMAPAR) could have a role in MFA signalling in the CA3. At MFA synapses, we can find calcium-permeable AMPAR (CP-AMPAR) and calcium-impermeable AMPAR (CI-AMPAR;Toth et al., 2000). MFB-CA3PC synapses only express CP-AMPAR. Whereas MFF-SLIN synapses express both CP-AMPARs and CI-AMPARs. Toth et al., 2000 found that when a high frequency stimulation (HFS) protocol is applied to MFB-CA3PC synapses, the response is facilitation or even long-term potentiation. In contrast, at MFF-SLIN synapses, there is no change or long-term depression (LTD). They evaluated AMPAR types and found the depressing synapse to be endowed with CP-AMPAR and the other with CI-AMPAR. Then a few years later, our lab discovered mGluR7 to play a role as the 'metaplastic switch' at CP-AMPAR (Pelkey et al., 2005). This meant when mGluR7 was inhibited, instead of LTD, the

synapse responded with LTP. Meaning, synapses with CI-AMPAR do not exhibit long-term depression (LTD), due to mGluR7 activity (Pelkey et al., 2005; Toth et al., 2000). Elfn1 recruits mGluR7 to the synapse, therefore, the presence of mGluR7 is dependent on Elfn1 activity and eliminating Elfn1 could have potentially significant changes to synaptic plasticity (Sylwestrak et al., 2012). Future experiments on Elfn1 KO mice would explore how players such as mGluR7, CI-AMAPAR, CP-AMPAR, and Elfn1 might be involved in the mechanisms of information transfer between the GC-CA3 network. *Could this difference in AMPA receptor types be the driving force behind the distinct coding strategies?* Our hypothesis is that in the absence of Elfn1, the transmission at SLIN synapses with CP-AMPARs would be affected, resulting in the abolishment of different coding strategies. Thus, this molecular approach could elucidate the mechanisms behind target-specific response to the same pre-synaptic stimuli.

Interneuron Subtype | Another approach to understanding how stratum lucidum interneurons apply different methods of synaptic transmission is by classifying the interneurons by their subtypes (Fishell & Kepecs, 2020; Parra et al., 1998). Interneurons are a diverse group of cells and notoriously difficult to classify. SLINs are no exception to that diversity (Que et al., 2021; Santana et al., 2013; Yuste, 2005). They exhibit diverse morphological characteristics, including various dendritic arborizations and axonal projections. This diversity provides them with the structure to extend to various targets within the CA3 and form networks to regulate activity in the region (Booker & Vida, 2018). Their inhibitory actions are crucial for maintaining the balance of excitation and inhibition within the hippocampal circuitry. Therefore, CA3 SLINs play an important role in regulating hippocampal firing patterns, ultimately impacting the flow of information within the hippocampus (Kamiya et al., 1996; Szabadics & Soltesz, 2009).

Despite the diversity, scientists have established methods to characterise interneurons based on the following: 1) morphology & location 2) electrophysiological properties 3) molecular markers 4) target connection 5) functional. Our focus is less on categorising all interneurons, but determining if their subtypes influence the way they transmit information. This type of categorisation could be useful as a *post-hoc* analysis. Given that biocytin was included in the intracellular solution for all recordings, a follow-up preliminary experiment could use the existing biocytin data and examine the filopodial morphology of the SLIN. Specifically, examination of the spine density, location, and connections of each SLIN subtype would be useful in this regard. The ultimate goal of this work would be to provide deeper insights in how the hippocampus processed information, essential for the proper functioning of the brain region.

Limitation Associated with Coding Strategies Clustering | One potential drawback with our current work is due to the methods we used to separate coding strategies. We separated sub-populations of coding strategies by eye. This leads to qualitative differences that contribute to experimenter bias. Given the limited dataset, visual separation is a simple method for preliminary data, but with a larger dataset more qualitative clustering methods would be applied to distinguish between sub-populations.

2.3.3 | Relevance to DG-CA3 Network & Future Experiments

What is important to the DG-CA3 Network? CA3 interneurons outnumber pyramidal cells by many magnitudes and contribute significant feedforward inhibition to CA3 excitatory cells (Acsády et al., 1998). Understanding MFF-SLIN synapses provides us with the missing piece to study the computations of the DG-CA3 network as a whole. We want to determine the coding strategies of MFF-SLIN synapses and how their methods of communication impacts the DG-CA3 network.

Future Directions | *What do these 3 different coding strategies mean for feedforward inhibition?* To answer this question, we would need to first validate these preliminary findings with a larger sample size. This study is the beginning of our evaluation of coding strategies in the CA3. It shows promising potential in using this methodology to uncover how information is transferred at MFF-SLIN synapses. However, the small sample size is a major limitation. First, when comparing MFF-SLIN sub-populations, one cell in each group is not enough to reliably separate into sub-populations, nor compare the kinetics between groups. This limitation also makes it difficult to have a meaningful discussion of how MFF-SLIN synapses function. Second, CA3-input types cannot be compared based on their responses to DCG-IV and NBQX given our sample size was limited to one cell that exhibited insensitivity of both DCG-IV and NBQX, which resulted in the two inputs being grouped together under "CA3 inputs." In the future, using the Elfn1 KO mice, along with increasing the sample size of WT animals would be essential in order to explore the network implications of various SLIN coding strategies on feedforward inhibition in the CA3 (Rossbroich et al., 2021).

2.4 | Conclusion

Despite recording challenges and low DCG-positive cells, this small sample shows promising data to the various ways MFF-SLIN synapses transfer information. Our preliminary findings in this thesis suggest that MFF-SLIN synapses employ 3 distinct coding strategies. One mechanism is insensitive to frequency, with the other 2 coding for changes in frequency in different ways. More experiments need to be conducted to further validate the strategies and elucidate their synaptic mechanisms. These findings

could provide a significant contribution to our understanding of feedforward inhibition within the DG-CA3 network.

2.5 | Methods

2.5.1 | Subject Details

For this study, we employed 13 C57BL/6 mice of both sexes, aged P21 - P42 from Charles River (Charles River, QC). Female mice were grouped-housed, while male mice were single-housed before experimental procedures. The housing room was on a 12 h-light and 12 h-dark cycle. Both sexes were provided with physical enrichments and *ad libitum* access to food and water. All experiments were performed in accordance with the guidelines set by the Canadian Council on Animal Care and all procedures were approved by the Animal Care and Veterinary Services at University of Ottawa.

2.5.2 | Acute Hippocampal Slice Preparation

Solutions

The solutions and methods were similar as those described in Chamberland et al., 2018. Artificial cerebrospinal fluid (aCSF) and sucrose-aCSF solutions were prepared the day of experiments. The aCSF contained (in mM): NaCl 124, $NaHCO_3$25, Glucose 10, KCl 2.5, $MgCl_2$ 1.2, $CaCl_2$ 1.2 (pH = 7.3, 305 mOsm). The sucrose-aCSF contained (in mM): NaCl 87, $NaHCO_3$ 25, Sucrose 75, Glucose 25, $MgCl_2$ 7, KCl 2.5, NaH_2PO_4 1.25, $CaCl_2$ 0.5 (pH = 7.3, 305 mOsm). It is notable that this solution included 1.2nM Ca2+, which is not the same as the 2.1nM Ca2+ that was previously used in Chamberland et al., 2018. The change was made to conduct experiments at more physiological Ca2+ levels and our unpublished data suggested cleaner recordings due to less signal contamination from CA3 collaterals (Kandel & Schwartz, 2014). The solutions were oxygenated by bubbling a gas mixture composed of 95% O_2 and 5% CO_2 for 15 minutes before being used for slice preparation. The aCSF-sucrose solution was cooled down by placing the beaker into liquid nitrogen. The solution was constantly stirred until it reached a slush-like consistency. It was then placed on ice and oxygenated before use.

Slicing

Mice were anaesthetised with liquid isoflurane and decapitated after a toe-reflex check. Their brains were quickly extracted and placed in the ice-cold sucrose-aCSF to perfuse and cool down for 5 minutes. The hemispheres were prepared with the ‘magic cut’ technique from Bischofberger et al., 2006 to provide the optimal angle for slicing (Bischofberger et al., 2006). This ‘magic cut' increases the probability that each slice

will have an intact full-length MF tract rather than fragmented MF segments across slices. Slices were cut to 300µm using a vibratome (Leica, VT1000s) in a cold, oxygenated sucrose-aCSF solution. The slices were then transferred to a 32 °C aCSF solution to incubate for 30 minutes. To note, during the study the slice incubation temperature was changed from 32°C to 37°C, which did not affect the recordings (data not shown). Data from both temperatures have been included in this thesis. The slices were then moved to room temperature and left to recover for 30 minutes before recordings.

2.5.3 |Whole-Cell Patch-Clamp Recordings

Recording Setup

The slices were transferred to a recording chamber that was perfused with constant fresh aCSF at a rate of ~ 2.5 mL/ minute. The chamber was located under a microscope equipped with variable objectives, that was also mounted on an airtable for stabilisation. Using the 4X air objective, the hippocampus and specifically the stratum lucidum layer was identified. Then with the 40X immersion objective, the stimulating electrode was placed within the hilus, along the granule cell layer and the recording electrode on cells within the stratum lucidum layer. Both were both glass micropipettes between the size of 2.5 MΩ - 6.0 MΩ. The stimulating electrode was filled with aCSF, containing (in mM): NaCl 124, $NaHCO_3$25, Glucose 10, KCl 2.5, $MgCl_2$ 2.5, $CaCl_2$ 1.2 (pH = 7.3, 315 mOsm). The recording electrode contained (in mM): K-Gluconate 120, KCl 20, HEPES 10, $MgCl_2$ 2, Mg_2ATP 2, Phosphocreatine 7, EGTA 0.6, NaGTP 0.3, and 0.4 % Biocytin (pH = ~7.2, ~315 mOsm). The biocytin concentration was initially used at 0.2 %, however it was increased to 0.4% during the project due to the fluorescence signal being too weak. Increasing the biocytin concentration changed the mOsm of the intracellular solution from ~300mOsm to ~315 mOsm, which did not impact the reliability of the electrophysiology data (data not shown). Data from both concentrations have been included in this thesis. The whole-cell recordings were performed clamped at -70mV from the acute slices.

Finding MF Responses

To find clean and fast MF EPSC responses, we moved the stimulating electrode along the granule cell layer in the hilus. The electrode was attached to a constant-current stimulus isolator (AMPI Isoflex stimulator from MicroProbes). If no response was found deeper in the hilus, we moved the electrode closer to the cell, along the extended section of the stratum lucidum layer within the hilus. If there was still no response after 20 minutes, a new cell was used in the same slice. After 2-3 cells in a slice, the slice was either discarded or flipped. Once a monosynaptic response was found, the stimulation was turned down until there was no response. Then, the stimulation was gradually

turned up until the most minimal stimulation response was observed. This process determined the minimal stimulation intensity that would be used for the remainder of the experiments. The access resistance (Ra) was monitored live throughout recordings. If it changed beyond ± 20% of the first protocol, the cell was either discarded during recording or after analysis. Sometimes an attempt to reopen by applying negative pressure was made, but it was not always successful.

Stimulation Protocols

The voltage-clamp stimulation protocol for stratum lucidum interneurons (SLIN) was as follows: A: 6x20Hz, B: 6x100Hz, C1: 5x20Hz + 1x100Hz and C2: 5x100Hz + 1x20Hz. Protocols A and B evaluated the difference between stimulation frequencies (high: 100Hz vs low: 20H), while the number of simulations remained constant (i.e. 6). Whereas protocols B and C considered the average stimulating frequency (120Hz) across a 6 stimulation train. Minimal stimulation was used to reduce the probability of activating CA3 collateral inputs that could contaminate MFA signals. The signals were acquired using an Axopatch 200B or 700B (Molecular Devices), low-pass filter at 2kHz, and digitised, at 10kHz with Digidata 1550B (Molecular Devices). Electrophysiological signals were acquired with a Multiclamp 700B amplifier (Molecular Devices). Data were low-pass filtered at 2 kHz and digitised at 10 kHz 206 with a Digidata 1440A. Recordings were performed with the Clampex 11.0 software. Electrophysiological data were analysed using Clampfit 10.2 and Prism 9.0.

Pharmacology

At the end of the recordings, (2S,1'R,2'R,3'R)-2-(2,3-dicarboxycyclopropyl)-glycine (DCG-IV) was applied to the recording chamber to confirm MFA inputs. DCG-IV is selective agonist for group II metabotropic glutamate receptors (mGluR2/3). The drug is used as a pharmacological confirmation of MFA signals because group II subtypes are solely expressed at MF synapses and the activation of these receptors reduces synaptic excitation (Pelkey et al., 2005; Yoshino et al., 1996). To confirm MFA inputs, 1µM DCG-IV was applied to the bath after the stimulation protocols (Pelkey et al., 2005). The literature on the concentration used for DCG-IV and percentage reduction after DCG-IV application varied between 0.5 nM to 0.1 µM and 25 - 80% (Yoshino et al., 1996; Dawson et al., 2000; Toth et al., 2000; Pelkey et al., 2005). The reduction from DCG-IV application was calculated *post-hoc*. In alignment with our lab's previous work (Pelkey et al., 2005; Toth et al., 2000), the initial selection criteria for confirming the cells had MFA input was a 50% reduction after DCG-IV application. However, due to the limited data of this study, we changed it to 49% to include one more cell to have one in each MFF-SLIN category. If there was no visible reduction observed with DCG-IV during recording, 10µM of (2,3-dioxo-6-nitro-7-sulfamoyl-

benzo[f]quinoxaline) (NBQX) was washed into the bath. NBQX is an AMPA receptor antagonist; reduction confirms glutamatergic excitation. Whereas no reduction indicated inputs were GABAergic.

2.5.4 |Electrophysiology Data Analysis

Analysis Software and Packages

Electrophysiological data was manually analysed with Clampfit 11.2 (Molecular Devices) and visualised by Prism 9 (Graphpad). The automated analysis was done in Python 3.11.0 using the following open source packages: pyABF (Harden, 2022) and Michael Lynn's github (Lynn, 2022). The packages helped read the proprietary .abf format and to extract the values from the files. The script was called AnalABF, with each new version dated and numbered. The Matplotlib package was used for plotting and visualisation.

Each analysed value was calculated from the average trace of each protocol. Every protocol had 20 sweeps, with an interval of 15 seconds between sweeps to avoid inducing long-term plasticity. The following values were automatically extracted. The amplitude of EPSCs was measured at the peak. They were detected by using the stimulation channel as a marker for the start of the peak search region, looking for a local maxima, the EPSC amplitude. The access resistance (Ra) and membrane resistance (Rm) were calculated using the access and membrane EPSC amplitude in the -5mV step before the stimulation. The paired-pulse ratio was measured by dividing the average response of the second peak amplitude with the first. The rise time was measured between the time of the peak amplitude and 95% of the rise time to baseline. The decay τ of EPSCs was measured from peak amplitude to baseline manually on Clampfit 11.2 (Molecular Devices).

Analysis Pipeline

1) Setup analysis-mapping (anal-map) to map the data files, order, and protocols to a specific cell. This mapping was also used to extract relevant data files for analysis.
2) Run the script to process the .abf files. No filtering was done during analysis, but sweeps with breakthrough action potentials were removed.
3) The following values were extracted and copied onto a .csv: **1)** Ra **2)** Rm **3)** Peak Amplitudes **4)** Rise Time
4) A 3x3 chart of each cell was created for visualisation with the following protocols: **1)** no-low **2)** minimal **3)** Protocol A **4)** Protocol B **5)** Protocol C1 **6)** Protocol C2 **7)** DCG-baseline **8)** DCG-last **9)** NBQX-last.
5) The cells were selected based on the inclusion criteria

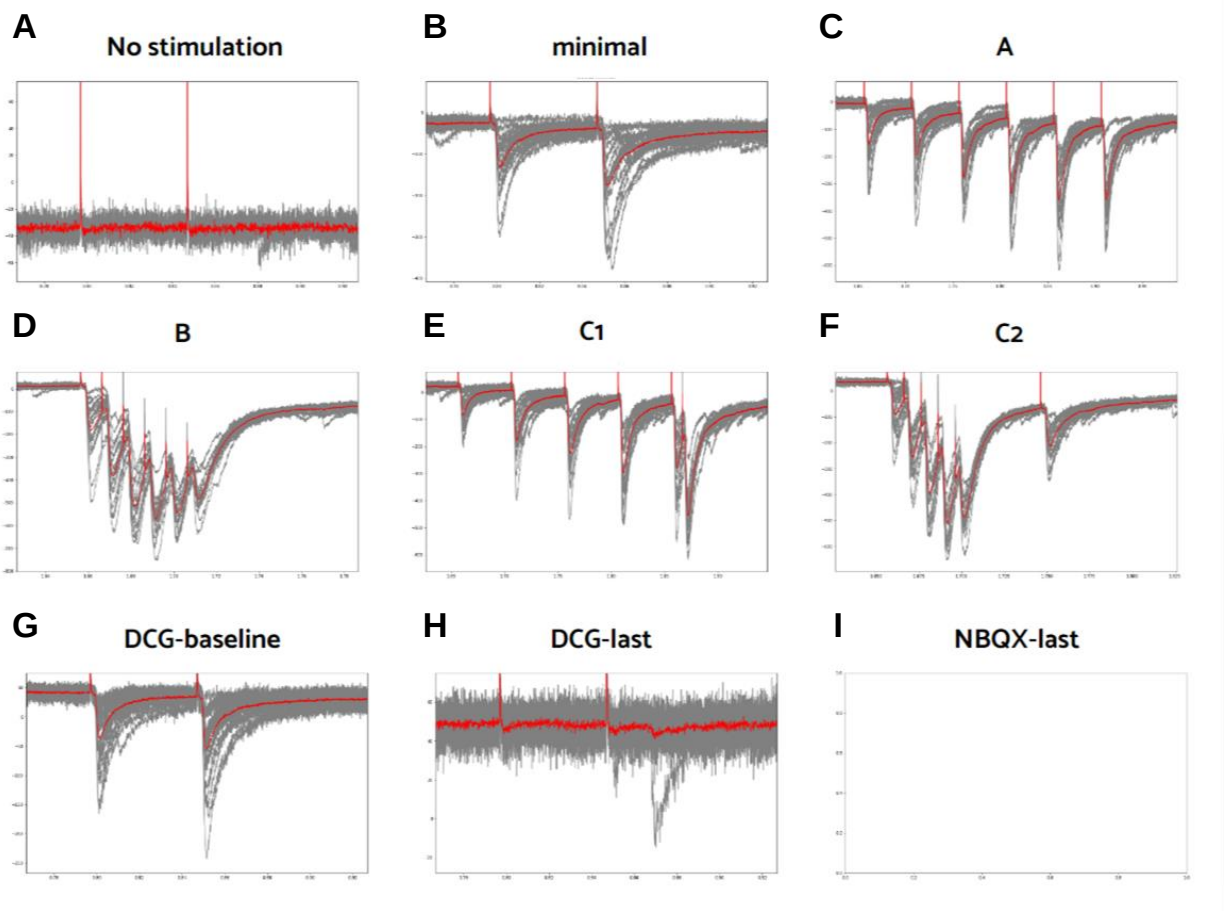

Figure 13 | 3x3 Chart Outputted from Analysis Script | **(A)** No stimulation or no-low protocol. Turned down stimulation until no response and turn up a smidge for minimal stimulation in B. **(B)** minimal stimulation of 50ms pair pulse recording. **(C)** Protocol A **(D)** Protocol B **(E)** Protocol C1 **(F)** Protocol C2 **(G)** DCG-baseline **(H)** DCG-last **(I)** NBQX-last. No recording because observed DCG-last reduction was close to 100%.

2.5.5 | Data Selection Criteria: Exceptions and Examples

Recordings that were included in the results in this report all met the following selection criteria:

1) Monosynaptic input **|** Monosynaptic input was determined by using a paired-pulse (PP) stimulation protocol with an interstimulus interval (ISI) of 50 ms. An ideal response has a fast rise time (3 +/- 2ms) with a clean and smooth exponential decay (Figure 13A). The holding amplitude remained between -100pA to 100 pA with Monosynaptic response is one way to demonstrate inputs are from MFAs and not other sources, like CA3 collaterals. There were some exceptions made on a case-by-case basis during Criteria 3.

2) "Stable" Ra throughout recordings, ≤30 MΩ | Stable access resistance (Ra) is imperative in VC experiments. The opening of a cell directly impacts how much current can pass through the patch of cell used for recording voltage currents. Therefore, if the Ra increases (i.e., cell closing), then this would impact how much current (i.e., smaller amplitude) is passing through the cell and detected by the recording electrode. Stability is determined by taking the Ra of the first protocol and all the following protocols have to fall within a +/- 20% range of that value (Figure 14E). The Ra of every protocol had to be under ≤30 MΩ. There were 2 exceptions:

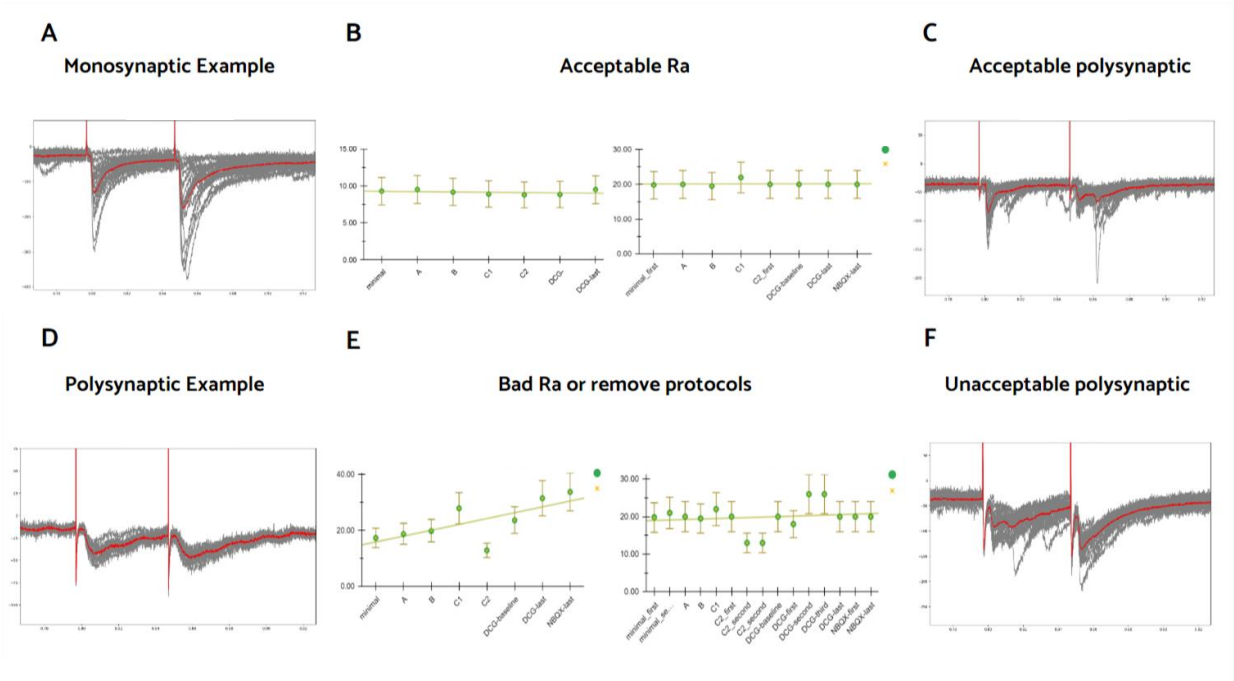

Figure 14 | Exclusion Criteria Examples | (A) Example of monosynaptic response during PP 50 ms stimulation. **(B)** Example of acceptable access resistance (Ra) throughout protocols. **(C)** Example of polysynaptic looking cell, but acceptable for data inclusion due to exponential decay and anomaly artefact influencing decay. **(D)** Example of polysynaptic response during PP 50 ms stimulation. **(E)** Examples of inacceptable access resistance (Ra) throughout protocols or that require removing protocols that were not analysed. **(F)** Example of polysynaptic looking cell, but not included in the data due to linear decay.

Exception 1: "Stable" is in quotations because only the protocols used for data were evaluated for Ra stability (Figure 14). This means the ones that were not used could have been outside this +/- 20% range.

Exception 2: Additionally, DCG-IV and NBQX protocols are compared to a PP ISI 50ms protocol after all the stimulation protocols called "DCG-IV baseline". The stimulation protocols affect the short-term plasticity of the recording, so a new baseline

is required to make the pharmacological comparison. For this reason, DCG-baseline is the new Ra value for the +/- 20% range and the Ra might not be the same "stable Ra" as the ones used for the stimulation protocols.

3) Visual Inspection | This allowed for detailed inspection of each cell and their responses, since every cell is different. From this discussion, some cells that did not fit exactly the previous two criteria were included. Here are a few examples

Example 1: A cell with an Ra value greater than 30 MΩ and outside the +/- 20% range (Figure 14). The value was at 32 MΩ and higher by 22% than the baseline Ra value. This cell was accepted into the dataset and the criteria value was changed to accommodate.

Example 2a: Bimodal-looking response (Figure 7C). This cell was determined not to be polysynaptic. The bimodal peaks were due to the horizontal jitter of individual responses that when averaged, looked bimodal.

Example 2b: This cell seems like it would be similar to Example 2a (Figure 7F). but with close inspection, the decay is more linear and less exponential, indicating a polysynaptic response.

References

Acsády, L., Kamondi, A., Sík, A., Freund, T., & Buzsáki, G. (1998). GABAergic Cells Are the Major Postsynaptic Targets of Mossy Fibers in the Rat Hippocampus. *The Journal of Neuroscience: The Official Journal of the Society for Neuroscience*, *18*(9), 3386–3403. https://doi.org/10.1523/JNEUROSCI.18-09-03386.1998

Andersen, P., Blackstad, T. W., & Lómo, T. (1966). Location and identification of excitatory synapses on hippoeampal pyramidal cells. *Experimental Brain Research. Experimentelle Hirnforschung. Experimentation Cerebrale*, *1*(3). https://doi.org/10.1007/bf00234344

Andersen, P., Morris, R., Amaral, D., Bliss, T., & O' Keefe, J. (2009). The Hippocampus Book. *The Hippocampus Book*, 1–852. https://doi.org/10.1093/ACPROF:OSO/9780195100273.001.0001

Arantius, J. C. (1923). De Humano Foetu Liber tertio editus, ac recognitus. Anatomicarum Observationum Liber, ac de Tumoribus Secundum Locos Affectos Liber. Venetiis: Apud …. *The Journal of Comparative Neurology*.

Asadi-Pooya, A. A., & Rostami, C. (2017). History of surgery for temporal lobe epilepsy. *Epilepsy & Behavior: E&B*, *70*(Pt A), 57–60. https://doi.org/10.1016/j.yebeh.2017.02.020

Atkinson, R. C., & Shiffrin, R. M. (1968). Human memory: A proposed system and its control processes. In K. W. Spence & J. T. Spence (Eds.), *Psychology of Learning and Motivation* (Vol. 2, pp. 89–195). Elsevier. https://doi.org/10.1016/s0079-7421(08)60422-3

Bear, M. F., & Malenka, R. C. (1994). Synaptic plasticity: LTP and LTD. *Current Opinion in Neurobiology*, *4*(3), 389–399. https://doi.org/10.1016/0959-4388(94)90101-5

Behrens, T. E. J., Muller, T. H., Whittington, J. C. R., Mark, S., Baram, A. B., Stachenfeld, K. L., & Kurth-Nelson, Z. (2018). What Is a Cognitive Map? Organizing Knowledge for Flexible Behavior. *Neuron*, *100*(2), 490–509. https://doi.org/10.1016/j.neuron.2018.10.002

Berdugo-Vega, G., Arias-Gil, G., López-Fernández, A., Artegiani, B., Wasielewska, J. M., Lee, C.-C., Lippert, M. T., Kempermann, G., Takagaki, K., & Calegari, F. (2020). Increasing neurogenesis refines hippocampal activity rejuvenating navigational learning strategies and contextual memory throughout life. *Nature Communications*, *11*(1), 135. https://doi.org/10.1038/s41467-019-14026-z

Bir, S. C., Ambekar, S., Kukreja, S., & Nanda, A. (2015). Julius Caesar Arantius (Giulio Cesare Aranzi, 1530-1589) and the hippocampus of the human brain: history behind the discovery. *Journal of Neurosurgery*, *122*(4), 971–975. https://doi.org/10.3171/2014.11.JNS132402

Bischofberger, J., Engel, D., Frotscher, M., & Jonas, P. (2006). Timing and efficacy of transmitter release at mossy fiber synapses in the hippocampal network. *Pflugers Archiv: European Journal of Physiology*, *453*(3), 361–372. https://doi.org/10.1007/s00424-006-0093-2

Bliss, T. V., & Lomo, T. (1973). Long-lasting potentiation of synaptic transmission in the dentate area of the anaesthetized rabbit following stimulation of the perforant path. *The Journal of Physiology*, *232*(2), 331–356. https://doi.org/10.1113/jphysiol.1973.sp010273

Booker, S. A., & Vida, I. (2018). Morphological diversity and connectivity of hippocampal interneurons. *Cell and Tissue Research*, *373*(3), 619–641. https://doi.org/10.1007/s00441-018-2882-2

Bouchekioua, Y., Blaisdell, A. P., Kosaki, Y., Tsutsui-Kimura, I., Craddock, P., Mimura, M., & Watanabe, S. (2021). Spatial inference without a cognitive map: the role of higher-order path integration. *Biological Reviews of the Cambridge Philosophical Society*, *96*(1), 52–65. https://doi.org/10.1111/brv.12645

Breedlove, M., & Watson, N. (2013). Biological psychology. Sinauer Associates Inc.

B Sakmann, A., & Neher, E. (2003). *Patch Clamp Techniques for Studying Ionic Channels in Excitable Membranes*. https://doi.org/10.1146/annurev.ph.46.030184.002323

Buzsáki, G. (2015, October 1). *Hippocampal sharp wave-ripple: A cognitive biomarker for episodic memory and planning - Buzsáki - 2015 - Hippocampus - Wiley Online Library*. John Wiley and Sons Inc. https://doi.org/10.1002/hipo.22488

Chamberland, S., Timofeeva, Y., Evstratova, A., Volynski, K., & Tóth, K. (2018). Action potential counting at giant mossy fiber terminals gates information transfer in the hippocampus. *Proceedings of the National Academy of Sciences of the United States of America*, *115*(28), 7434–7439. https://doi.org/10.1073/pnas.1720659115

Citri, A., & Malenka, R. C. (2008). Synaptic plasticity: multiple forms, functions, and mechanisms. *Neuropsychopharmacology: Official Publication of the American College of Neuropsychopharmacology*, *33*(1), 18–41. https://doi.org/10.1038/sj.npp.1301559

Clemenson, G. D., Maselli, A., Fiannaca, A. J., Miller, A., & Gonzalez-Franco, M. (2021). Rethinking GPS navigation: creating cognitive maps through auditory clues. *Scientific Reports*, *11*(1), 7764. https://doi.org/10.1038/s41598-021-87148-4

Corkin, S. (1984). Lasting consequences of bilateral medial temporal lobectomy: Clinical course and experimental findings in H.m. *Seminars in Neurology*, *4*(02), 249–259. https://doi.org/10.1055/s-2008-1041556

Corkin, S., Amaral, D. G., González, R. G., Johnson, K. A., & Hyman, B. T. (1997). H. M.'s medial temporal lobe lesion: findings from magnetic resonance imaging. *The Journal of Neuroscience: The Official Journal of the Society for Neuroscience*, *17*(10), 3964–3979. https://doi.org/10.1523/JNEUROSCI.17-10-03964.1997

Davidson, T. J., Kloosterman, F., & Wilson, M. A. (2009). Hippocampal replay of extended experience. *Neuron*, *63*(4), 497–507. https://doi.org/10.1016/j.neuron.2009.07.027

Dawson, L., Chadha, A., Megalou, M., & Duty, S. (2000). The group II metabotropic glutamate receptor agonist, DCG-IV, alleviates akinesia following intranigral or intraventricular administration in the reserpine-treated rat. *British Journal of Pharmacology*, *129*(3), 541–546. https://doi.org/10.1038/sj.bjp.0703105

Denker, A., & Rizzoli, S. O. (2010). Synaptic vesicle pools: an update. *Frontiers in Synaptic Neuroscience*, *2*, 135. https://doi.org/10.3389/fnsyn.2010.00135

Diamantaki, M., Frey, M., Berens, P., Preston-Ferrer, P., & Burgalossi, A. (2016). Sparse activity of identified dentate granule cells during spatial exploration. *eLife*, *5*, e20252. https://doi.org/10.7554/eLife.20252

Dunn, H. A., Patil, D. N., Cao, Y., Orlandi, C., & Martemyanov, K. A. (2018). Synaptic adhesion protein ELFN1 is a selective allosteric modulator of group III metabotropic glutamate receptors in trans. *Proceedings of the National Academy of Sciences of the United States of America*, *115*(19), 5022–5027. https://doi.org/10.1073/pnas.1722498115

Engelhardt, E. (2016). Hippocampus discovery First steps. *Dementia & Neuropsychologia*, *10*(1), 58–62. https://doi.org/10.1590/S1980-57642016DN10100011

Esch, H. E., & Burns, J. E. (1995). Honeybees use optic flow to measure the distance of a food source. *Die Naturwissenschaften*, *82*(1), 38–40. https://doi.org/10.1007/BF01167870

Fishell, G., & Kepecs, A. (2020). Interneuron Types as Attractors and Controllers. *Annual Review of Neuroscience*, *43*, 1–30. https://doi.org/10.1146/annurev-neuro-070918-050421

Förster, E., Zhao, S., & Frotscher, M. (2006). Laminating the hippocampus. *Nature Reviews. Neuroscience*, *7*(4), 259–267. https://doi.org/10.1038/nrn1882

Fyhn, M., Hafting, T., Treves, A., Moser, M.-B., & Moser, E. I. (2007). Hippocampal remapping and grid realignment in entorhinal cortex. *Nature*, *446*(7132), 190–194. https://doi.org/10.1038/nature05601

Garcia-Lopez, P., Garcia-Marin, V., & Freire, M. (2010). The histological slides and drawings of cajal. *Frontiers in Neuroanatomy*, *4*, 9. https://doi.org/10.3389/neuro.05.009.2010

Gillespie, A. K., Astudillo Maya, D. A., Denovellis, E. L., Liu, D. F., Kastner, D. B., Coulter, M. E., Roumis, D. K., Eden, U. T., & Frank, L. M. (2021). Hippocampal replay reflects specific past experiences rather than a plan for subsequent choice. *Neuron*, *109*(19), 3149–3163.e6. https://doi.org/10.1016/j.neuron.2021.07.029

Golgi, C. Sulla fina anatomia degli organi centrali del sistema nervoso. Reggio-Emilia: S. Calderini e Figlio; 1885.

Guo, J., Ge, J.-L., Hao, M., Sun, Z.-C., Wu, X.-S., Zhu, J.-B., Wang, W., Yao, P.-T., Lin, W., & Xue, L. (2015). A Three-Pool Model Dissecting Readily Releasable Pool Replenishment at the Calyx of Held. *Scientific Reports*, *5*(1), 9517. https://doi.org/10.1038/srep09517

Hafting, T., Fyhn, M., Molden, S., Moser, M.-B., & Moser, E. I. (2005). Microstructure of a spatial map in the entorhinal cortex. *Nature*, *436*(7052), 801–806. https://doi.org/10.1038/nature03721

Hodgkin, A. L., & Huxley, A. F. (1952). A quantitative description of membrane current and its application to conduction and excitation in nerve. *The Journal of Physiology*, *117*(4), 500–544. https://doi.org/10.1113/jphysiol.1952.sp004764

Jackman, S. L., & Regehr, W. G. (2017). The Mechanisms and Functions of Synaptic Facilitation. *Neuron*, *94*(3), 447–464. https://doi.org/10.1016/j.neuron.2017.02.047

Kandel, E., & Schwartz, J. (2014). In Principles of Neural Science (5th ed., pp. 1261–1275). McGraw-Hill Professional Publishing.

Kamiya, H., Shinozaki, H., & Yamamoto, C. (1996). Activation of metabotropic glutamate receptor type 2/3 suppresses transmission at rat hippocampal mossy fibre synapses. *The Journal of Physiology*, *493 (Pt 2)*(Pt 2), 447–455. https://doi.org/10.1113/jphysiol.1996.sp021395

Kjelstrup, K. G., Tuvnes, F. A., Steffenach, H.-A., Murison, R., Moser, E. I., & Moser, M.-B. (2002). Reduced fear expression after lesions of the ventral hippocampus. *Proceedings of the National Academy of Sciences of the United States of America*, *99*(16), 10825–10830. https://doi.org/10.1073/pnas.152112399

Klein, J. (2017, February 17). Hunched Over a Microscope, He Sketched the Secrets of How the Brain Works. *The New York Times*. https://www.nytimes.com/2017/02/17/science/santiago-ramon-y-cajal-beautiful-brain.html

Krueppel, R., Remy, S., & Beck, H. (2011). Dendritic Integration in Hippocampal Dentate Granule Cells. *Neuron*, *71*(3), 512–528. https://doi.org/10.1016/j.neuron.2011.05.043

Kumar, R., & Yeragani, V. K. (2011). Penfield - A great explorer of psyche-soma-neuroscience. *Indian Journal of Psychiatry*, *53*(3), 276–278. https://doi.org/10.4103/0019-5545.86826

Lashley, K. S. (1929). *Brain mechanisms and intelligence: A quantitative study of injuries to the brain*. psycnet.apa.org. https://psycnet-apa-org.proxy.bib.uottawa.ca/record/2004-16230-000

Lazarov, O., & Hollands, C. (2016). Hippocampal neurogenesis: Learning to remember. *Progress in Neurobiology*, *138-140*, 1–18. https://doi.org/10.1016/j.pneurobio.2015.12.006

Lewis, F. T. (1923). The significance of the termHippocampus. *The Journal of Comparative Neurology*, *35*(3), 213–230. https://books.google.com/books?hl=en&lr=&id=OpBNAAAAYAAJ&oi=fnd&pg=PA213&dq=Lewis+F+T+(1923)+The+significance+of+the+termHippocampus+The+Journal+of+Comparative+Neurology+35(3)+213-230&ots=BLNY4vBqIF&sig=_CIVKk7TovnVt9dJ49ezK305BCE

Lüscher, C., & Malenka, R. C. (2012). NMDA receptor-dependent long-term potentiation and long-term depression (LTP/LTD). *Cold Spring Harbor Perspectives in Biology*, *4*(6). https://doi.org/10.1101/cshperspect.a005710

Maccaferri, G., Tóth, K., & McBain, C. J. (1998). Target-Specific Expression of Presynaptic Mossy Fiber Plasticity. *Science*, *279*(5355), 1368–1371. https://doi.org/10.1126/science.279.5355.1368

Malenka, R. C. (2003). The long-term potential of LTP. *Nature Reviews. Neuroscience*, *4*(11), 923–926. https://doi.org/10.1038/nrn1258

Malenka, R. C., & Bear, M. F. (2004). LTP and LTD: an embarrassment of riches. *Neuron*, *44*(1), 5–21. https://doi.org/10.1016/j.neuron.2004.09.012

Martin, E. A., Woodruff, D., Rawson, R. L., & Williams, M. E. (2017). Examining Hippocampal Mossy Fiber Synapses by 3D Electron Microscopy in Wildtype and Kirrel3 Knockout Mice. *eNeuro*, *4*(3), ENEURO.0088–17.2017. https://doi.org/10.1523/ENEURO.0088-17.2017

M Carthy, J. G. (1898). A New Dissection showing the Internal Gross Anatomy of the Hippocampus major. *Journal of Anatomy and Physiology*, *33*(Pt 1), 76–81. https://www.ncbi.nlm.nih.gov/pubmed/17232360

McNaughton, B. L., Battaglia, F. P., Jensen, O., Moser, E. I., & Moser, M.-B. (2006). Path integration and the neural basis of the "cognitive map." *Nature Reviews. Neuroscience*, *7*(8), 663–678. https://doi.org/10.1038/nrn1932

Miller, A. M. P., Jacob, A. D., Ramsaran, A. I., De Snoo, M. L., Josselyn, S. A., & Frankland, P. W. (2023). Emergence of a predictive model in the hippocampus. *Neuron*, *111*(12), 1952–1965.e5. https://doi.org/10.1016/j.neuron.2023.03.011

Milner, B. (1959). The memory defect in bilateral hippocampal lesions. *Psychiatric Research Reports*, *11*, 43–58. https://www.ncbi.nlm.nih.gov/pubmed/14422670

Milner, B. (1962). Study of short-term memory and intracarotid injection of sodium amytal. *Transactions of the American Neurological Association*, *87*, 224–226. https://cir.nii.ac.jp/crid/1570572699738143232

Milner, B. (1966). Amnesia following operation on the temporal lobes. *Amnesia*, 109–133. https://ci.nii.ac.jp/naid/10008101181/

Milner, B., Corkin, S., & Teuber, H. L. (1968). Further analysis of the hippocampal amnesic syndrome: 14-year follow-up study of HM. *Neuropsychologia*. https://www.sciencedirect.com/science/article/pii/0028393268900213?casa_token=2z-_2NW6W48AAAAA:Qq-ySni1B0TZDQTpC9Y9ETjPZsoehKMdbXdymCZZSlUa92xL_pBxfn8C3NvqtYbjbA7GFZWDmw

Molnar, C., & Gair, J. (2015a). 16.1 Neurons and Glial Cells. In *Concepts of Biology - 1st Canadian Edition*. BCcampus. https://opentextbc.ca/biology/chapter/16-1-neurons-and-glial-cells/

Molnar, C., & Gair, J. (2015b). 16.2 how neurons communicate. In *Concepts of Biology - 1st Canadian Edition*. BCcampus. https://opentextbc.ca/biology/chapter/16-2-how-neurons-communicate/

Moser, E. I., Kropff, E., & Moser, M. B. (2008). Place cells, grid cells, and the brain's spatial representation system. In *Annual Review of Neuroscience* (Vol. 31, pp. 69–89). Annual Reviews. https://doi.org/10.1146/annurev.neuro.31.061307.090723

Moser, E. I., Moser, M.-B., & McNaughton, B. L. (2017). Spatial representation in the hippocampal formation: a history. *Nature Neuroscience*, *20*(11), 1448–1464. https://doi.org/10.1038/nn.4653

Muñoz-López, M. (2015). Past, present, and future in hippocampal formation and memory research. *Hippocampus*, *25*(6), 726–730. https://doi.org/10.1002/hipo.22452

Neves, G., Cooke, S. F., & Bliss, T. V. P. (2012). Synaptic plasticity, memory and the hippocampus: a neural network approach to causality. *Nature Reviews. Neuroscience*, *9*(1), 65–75. https://doi.org/10.1038/nrn2303

Nicoll, R. A. (2017). A Brief History of Long-Term Potentiation. *Neuron*, *93*(2), 281–290. https://doi.org/10.1016/j.neuron.2016.12.015

Nicoll, R. A., & Schmitz, D. (2005). Synaptic plasticity at hippocampal mossy fibre synapses. *Nature Reviews. Neuroscience*, *6*(11), 863–876. https://doi.org/10.1038/nrn1786

Nikova, A., & Birbilis, T. (2017). The Basic Steps of Evolution of Brain Surgery. *Maedica*, *12*(4), 297–305. https://www.ncbi.nlm.nih.gov/pubmed/29610595

O'Keefe, J. (1976). Place units in the hippocampus of the freely moving rat. *Experimental Neurology*, *51*(1), 78–109. https://doi.org/10.1016/0014-4886(76)90055-8

O'Keefe, J., & Dostrovsky, J. (1971). The hippocampus as a spatial map. Preliminary evidence from unit activity in the freely-moving rat. *Brain Research*, *34*(1), 171–175. https://doi.org/10.1016/0006-8993(71)90358-1

O'Keefe, J., & Nadel, L. (1978). *The Hippocampus as a Cognitive Map*. 570. https://discovery.ucl.ac.uk/id/eprint/10103569/

Ólafsdóttir, H. F., Bush, D., & Barry, C. (2018). The Role of Hippocampal Replay in Memory and Planning. *Current Biology: CB*, *28*(1), R37–R50. https://doi.org/10.1016/j.cub.2017.10.073

Parra, P., Gulyás, A. I., & Miles, R. (1998). How Many Subtypes of Inhibitory Cells in the Hippocampus? *Neuron*, *20*(5), 983–993. https://doi.org/10.1016/S0896-6273(00)80479-1

Pavlov, I. P. (1927). *Conditioned reflexes: an investigation of the physiological activity of the cerebral cortex. 430*. https://psycnet.apa.org/fulltext/1927-02531-000.pdf

Pelkey, K. A., Lavezzari, G., Racca, C., Roche, K. W., & McBain, C. J. (2005). mGluR7 Is a Metaplastic Switch Controlling Bidirectional Plasticity of Feedforward Inhibition. *Neuron*, *46*(1), 89–102. https://doi.org/10.1016/j.neuron.2005.02.011

Penfield, W., & Gage, L. (1933). CEREBRAL LOCALIZATION OF EPILEPTIC MANIFESTATIONS. *Archives of Neurology & Psychiatry*, *30*(4), 709–727. https://doi.org/10.1001/archneurpsyc.1933.02240160009001

Penfield, W., & Milner, B. (1958). Memory deficit produced by bilateral lesions in the hippocampal zone. *A.M.A. Archives of Neurology and Psychiatry*, *79*(5), 475–497. https://doi.org/10.1001/archneurpsyc.1958.02340050003001

Purves, D., Augustine, G. J., Fitzpatrick, D., Katz, L. C., LaMantia, A.-S., McNamara, J. O., & Mark Williams, S. (2001a). *Excitatory and Inhibitory Postsynaptic Potentials*. Sinauer Associates. https://www.ncbi.nlm.nih.gov/books/NBK11117/

Purves, D., Augustine, G. J., Fitzpatrick, D., Katz, L. C., LaMantia, A.-S., McNamara, J. O., & Mark Williams, S. (2001b). *Neuroscience*. Sinauer Associates. https://www.ncbi.nlm.nih.gov/books/NBK10799/

Purves, D., Augustine, G. J., Fitzpatrick, D., Katz, L. C., LaMantia, A.-S., McNamara, J. O., & Mark Williams, S. (2001c). *Neurotransmitter Release and Removal*. Sinauer Associates. https://www.ncbi.nlm.nih.gov/books/NBK11106/

Que, L., Lukacsovich, D., Luo, W., & Földy, C. (2021). Transcriptional and morphological profiling of parvalbumin interneuron subpopulations in the mouse hippocampus. *Nature Communications*, *12*(1), 1–15. https://doi.org/10.1038/s41467-020-20328-4

Ramón y Cajal, S. (1899). *Textura del sistema nervioso del hombre y de los vertebrados : estudios sobre el plan estructural y composición histológica de los centros nerviosos adicionados de consideraciones fisiológicas fundadas en los nuevos descubrimientos. Volumen I*. https://digibug.ugr.es/handle/10481/69713

Rebola, N., Carta, M., & Mulle, C. (2017). Operation and plasticity of hippocampal CA3 circuits: implications for memory encoding. *Nature Reviews. Neuroscience*, *18*(4), 208–220. https://doi.org/10.1038/nrn.2017.10

Richards, B. A., & Frankland, P. W. (2017). The Persistence and Transience of Memory. *Neuron*, *94*(6), 1071–1084. https://doi.org/10.1016/j.neuron.2017.04.037

Rossbroich, J., Trotter, D., Beninger, J., Tóth, K., & Naud, R. (2021). Linear-nonlinear cascades capture synaptic dynamics. *PLoS Computational Biology*, *17*(3), e1008013. https://doi.org/10.1371/journal.pcbi.1008013

Santana, R., McGarry, L., Bielza, C., Larrañaga, P., & Yuste, R. (2013). Classification of neocortical interneurons using affinity propagation. *Frontiers in Neural Circuits*, *0*(DEC), 185. https://doi.org/10.3389/fncir.2013.00185

Schwiening, C. J. (2012). A brief historical perspective: Hodgkin and Huxley. *The Journal of Physiology*, *590*(11), 2571–2575. https://doi.org/10.1113/jphysiol.2012.230458

Scoville, W. B., & Milner, B. (1957). Loss of recent memory after bilateral hippocampal lesions. *Journal of Neurology, Neurosurgery, and Psychiatry*, *20*(1), 11–21. https://doi.org/10.1136/jnnp.20.1.11

Segev, A., Garcia-Oscos, F., & Kourrich, S. (2016). Whole-cell Patch-clamp Recordings in Brain Slices. *Journal of Visualized Experiments: JoVE*, *112*. https://doi.org/10.3791/54024

Skinner, B. F. (1963). Operant behavior. *The American Psychologist*, *18*(8), 503–515. https://doi.org/10.1037/h0045185

Sotelo, C. (2003). Viewing the brain through the master hand of Ramón y Cajal. *Nature Reviews. Neuroscience*, *4*(1), 71–77. https://doi.org/10.1038/nrn1010

Squire, L. R. (2009). The legacy of patient H.M. for neuroscience. *Neuron*, *61*(1), 6–9. https://doi.org/10.1016/j.neuron.2008.12.023

Squire, L. R., & Wixted, J. T. (2011). The cognitive neuroscience of human memory since H.M. *Annual Review of Neuroscience*, *34*, 259–288. https://doi.org/10.1146/annurev-neuro-061010-113720

Stachniak, T. J., Sylwestrak, E. L., Scheiffele, P., Hall, B. J., & Ghosh, A. (2019). Elfn1-Induced Constitutive Activation of mGluR7 Determines Frequency-Dependent

Recruitment of Somatostatin Interneurons. *The Journal of Neuroscience: The Official Journal of the Society for Neuroscience*, *39*(23), 4461–4474. https://doi.org/10.1523/JNEUROSCI.2276-18.2019

Sylwestrak, E. L., & Ghosh, A. (2012, October 26). *Elfn1 Regulates Target-Specific Release Probability at CA1-Interneuron Synapses | Science*. American Association for the Advancement of Science. https://doi.org/10.1126/SCIENCE.1222482

Szabadics, J., & Soltesz, I. (2009). Functional Specificity of Mossy Fiber Innervation of GABAergic Cells in the Hippocampus. *The Journal of Neuroscience: The Official Journal of the Society for Neuroscience*, *29*(13), 4239–4251. https://doi.org/10.1523/JNEUROSCI.5390-08.2009

Tolman, E. C. (1948). Cognitive maps in rats and men. *Psychological Review*, *55*(4), 189–208. https://doi.org/10.1037/h0061626

Tomioka, N. H., Yasuda, H., Miyamoto, H., Hatayama, M., Morimura, N., Matsumoto, Y., Suzuki, T., Odagawa, M., Odaka, Y. S., Iwayama, Y., Won Um, J., Ko, J., Inoue, Y., Kaneko, S., Hirose, S., Yamada, K., Yoshikawa, T., Yamakawa, K., & Aruga, J. (2014). Elfn1 recruits presynaptic mGluR7 in trans and its loss results in seizures. *Nature Communications*, *5*(1), 4501. https://doi.org/10.1038/ncomms5501

Torborg, C. L., Nakashiba, T., Tonegawa, S., & McBain, C. J. (2010). Control of CA3 Output by Feedforward Inhibition Despite Developmental Changes in the Excitation–Inhibition Balance. *The Journal of Neuroscience: The Official Journal of the Society for Neuroscience*, *30*(46), 15628–15637. https://doi.org/10.1523/JNEUROSCI.3099-10.2010

Tóth, K., & McBain, C. J. (1998). Afferent-specific innervation of two distinct AMPA receptor subtypes on single hippocampal interneurons. *Nature Neuroscience*, *1*(7), 572–578. https://doi.org/10.1038/2807

Toth, K., Suares, G., Lawrence, J. J., Philips-Tansey, E., & McBain, C. J. (2000). Differential Mechanisms of Transmission at Three Types of Mossy Fiber Synapse. *The Journal of Neuroscience: The Official Journal of the Society for Neuroscience*, *20*(22), 8279–8289. https://doi.org/10.1523/JNEUROSCI.20-22-08279.2000

Volianskis, A., Collingridge, G. L., & Jensen, M. S. (2013). The roles of STP and LTP in synaptic encoding. *PeerJ*, *1*, e3. https://doi.org/10.7717/peerj.3

Westra, M., Gutierrez, Y., & MacGillavry, H. D. (2021). Contribution of membrane lipids to postsynaptic protein organization. *Frontiers in Synaptic Neuroscience*, *13*, 790773. https://doi.org/10.3389/fnsyn.2021.790773

Wittlinger, M., Wehner, R., & Wolf, H. (2006). The Ant Odometer: Stepping on Stilts and Stumps. *Science*, *312*(5782), 1965–1967. https://doi.org/10.1126/science.1126912

Wittlinger, M., Wehner, R., & Wolf, H. (2007). The desert ant odometer: a stride integrator that accounts for stride length and walking speed. *The Journal of Experimental Biology*, *210*(2), 198–207. https://doi.org/10.1242/jeb.02657

Wolf, H. (2011). Odometry and insect navigation. *The Journal of Experimental Biology*, *214*(10), 1629–1641. https://doi.org/10.1242/jeb.038570

Xu, W., & Südhof, T. C. (2013). A neural circuit for memory specificity and generalization. *Science*. https://doi.org/10.1126/science.1229534

Yamada, Y., Mibe, Y., Yamamoto, Y., Ito, K., Heim, O., & Hiryu, S. (2020). Modulation of acoustic navigation behaviour by spatial learning in the echolocating bat Rhinolophus ferrumequinum nippon. *Scientific Reports*, *10*(1), 10751. https://doi.org/10.1038/s41598-020-67470-z

Yonelinas, A. P., Ranganath, C., Ekstrom, A. D., & Wiltgen, B. J. (2019). A contextual binding theory of episodic memory: systems consolidation reconsidered. *Nature Reviews. Neuroscience*, *20*(6), 364–375. https://doi.org/10.1038/s41583-019-0150-4

Yoshino, M., Sawada, S., Yamamoto, C., & Kamiya, H. (1996). A metabotropic glutamate receptor agonist DCG-IV suppresses synaptic transmission at mossy fiber pathway of the guinea pig hippocampus. *Neuroscience Letters*, *207*(1), 70–72. https://doi.org/10.1016/0304-3940(96)12486-1

Yuste, R. (2005). Origin and Classification of Neocortical Interneurons. *Neuron*, *48*(4), 524–527. https://doi.org/10.1016/j.neuron.2005.11.012